DIPLOMARBEIT

Titel der Diplomarbeit

Visualization of ApoER2 and Vldlr During the Ligand-Mediated Signal-Transduction

verfasst von

Roland Kuttner

angestrebter akademischer Grad

Magister der Naturwissenschaften (Mag.rer.nat.)

Wien, 2013

Index

Abstract

The characteristic *Reeler* phenotype and the well studied Reelin signalling pathway are a long established model system for the study of the development of the mammalian brain.

Apolipoprotein E receptor 2 (ApoER2) and very low density lipoprotein receptor (Vldlr) have been shown to be integral parts of the Reelin signalling pathway, as they interact with Reelin and transduce the signal downstream. The working model for the signalling pathway is that upon binding of Reelin to either ApoER2 or Vldlr, the receptors dimerize, bind the intracellular adapter protein Disabled homolog 1 (Dab1) which dimerizes as well and is subsequently phosphorylated. However neither of these dimerizations have ever been shown directly.

In this study cell lines expressing fluorescently tagged murine ApoER2 and Vldlr were established, in order to study the mechanisms of the Reelin pathway in a live cell model at the molecular level. A total of ten different fluorescent tags were utilized in conjunction with each of the receptors in the attempt to produce an adequate cell line. These variants differ by the use of 4 alternative fluorescent proteins (mCherry, EGFP, TagGFP2 or TagRFP) as well as 4 types of small linker sequences.

Specifically Hek 293 cells with stable expression of TagGFP2 - tagged ApoER2 (cell line GA IV) or Vldlr (cell line GV I) displayed the most promising properties for fluorescence imaging microscopy applications.

Using these established cell lines distinct interactions of fluorescently tagged Dab1 with ApoER2 and Vldlr were shown. Dab1 colocalizes with Vldlr next to the plasma membrane, but does not do so with ApoER2.

Furthermore the suggested dimerization or clustering of ApoER2 and Vldlr upon the interaction with Reelin was studied using anisotropy imaging. Reelin stimulation caused a decrease in anisotropy in GA IV cells (ApoER2), indicating a homo - FRET (Förster resonance energy transfer) event due to clustering of the fluorescently tagged receptor. However this could not be demonstrated in GV I cells (Vldlr). While more repetitions of these experiments are required for definitive conclusions, the data presented here should serve as a reasonable indication, that Reelin indeed causes ApoER2 clustering upon binding.

With the tools set up in these experiments in depth studies of the Reelin signalling pathway using a variety of fluorescence imaging methods can be performed.

Introduction

ApoER2

Apolipoprotein E receptor 2 (ApoER2) is a member of the LDL (low density lipoprotein) receptor family. It consists of a cytoplasmic domain 4, 5 or 8 LDL receptor class A repeats (LA repeats), a furin cleavage site, an EGF precursor homology domain, an O-linked sugar domain, the transmembrane region and a proline rich insert in the cytoplasmic domain[1]. In the following experiments the *Mus musculs* variant with 5 LA repeats and the proline rich insert was used[2].

Vldlr

The very low density lipoprotein receptor (Vldlr) not only belongs to the LDL receptor family but is remarkably similar to the LDL receptor[1,3]. It consists of a cytoplasmic domain, 8 LDL receptor class A repeats (LA repeats), an EGF precursor homology domain, an O-linked sugar domain (OLSD) which can be deleted from some variants, the transmembrane region and the cytoplasmic domain. Here the *Mus musculs* Vldlr variant lacking the OLSD was used

Reelin Signalling Pathway

Reelin, which is produced by Cajal-Retzius cells, plays an integral role in the correct migration and positioning of cortical plate neurons during embryonic brain development of mammals[4]. Upon the disruption of the Reelin signalling pathway, as happens in animals lacking a functional Reelin gene, various abnormal tissue formations in the brain, such as an inversion of the layers of the neural cortex can be observed[5] (*Reeler* phenotype in mice). This dysplasia is characterized by the failure of neurons to split the preplate upon their migration from the subventricular zone to the marginal zone resulting in a seemingly inverted, disorganized arrangement of the layers of the neocortex.

ApoER2 and Vldlr are both receptors for Reelin[6,7]. In ApoER2 (-/-), Vldlr (-/-) double knockout mice similar abnormal brain developments to the *Reeler* phenotype can be observed[8], showing that they are integral parts of the signalling pathway. In mice lacking only one of the two receptors, a milder phenotype can be observed, suggesting that ApoER2 and Vldlr transduce the Reelin signal in a similar way. However while ApoER2 is needed for migration of neurons in later stages of the development, Vldlr has been

hypothesized to work as a Reelin mediated stop signal, once migrating neurons have reached their destination[9,10].

Binding of Reelin to ApoER2 \ Vldlr is followed by phosphorylation of Disabled homolog 1 (Dab1)[11–13]. Dab 1 phosphorlyation on tyrosines 198 and 220[14], is mediated by a Src family non receptor kinase[15,16]. These phosphorylations are dependant on the *NFDNPXY* motive of the ApoER2 \ Vldlr intracellular domain, a motive that binds Dab1 but is also associated with the clathrin mediated endocytosis in other receptors of the LDL receptor family[17,18,19].

Upon binding ApoER2 \ Vldlr - Reelin complexes are also internalized. While Vldlr, which is present throughout the plasma membrane, is internalized rather fast ApoER2 is internalized much slower, because of its association with lipid rafts. After endocytosis Vldlr is recycled back to the cytoplasmic membrane, while ApoER2 is degraded in lysosomes[20].

Dimerization of ApoER2 or Vldlr due to binding with a Rap-Fc construct or polyclonal antibodies recognizing the ligand binding domain of the receptor, alone can induce the phosphorylation of Dab1, mimicking stimulation with Reelin[21]. Similarly Dab1 dimerization is capable of inducing downstream reactions.

These reactions include the activation of phosphoinositide 3-kinase (PI3K) [22], which inhibits glycogen synthase kinase 3 β (GSK3β) as well as the phosphorylation of n-cofilin and together could account for possible changes in protein expression as well as the migrational behaviour of the neurons[23].

The goals of my diploma work were to establish possibilities to image the processes during the ligand - receptor interaction. This was attempted by establishing and examining different fusion proteins of fluorescent proteins (FPs) and components of the Reelin signalling pathway (ApoER2, Vldlr, Dab1).

FRET

Förster resonance energy transfer (FRET) is a non radiative energy transfer resulting in an excitation between two fluophores[24–26]. Electrons on the donor fluophore are elevated into higher energy states with energy, usually provided in the form of photons. Normally the electron on the donor fluophore then relaxes back to its ground stage, emitting a photon of longer wavelength than the one used for the excitation. If however a suitable second fluophore is in close vicinity, the energy may be transferred to this acceptor

molecule. FRET therefore relies on a long range dipole - dipole energy transfer highly dependant upon the distance of the two fluophores.

$$k_{ET} = \frac{1}{\tau_D}(\frac{R_0}{R})^6$$ (1)

Equation (1) describes these properties with the average rate of FRET k_{ET} being dependant on the sixth power of the fraction $\frac{R_0}{R}$ with R_0 being the Förster distance of the donor acceptor pair, R the actual donor acceptor distance and τ_D being the fluorescence life time of the donor with no potential FRET partner present

$$R_0^6 \propto \frac{\kappa^2 \phi_D}{n^4}\Gamma$$ (2)

The Förster distance R_0 is the distance at which 50% of donors transfer energy to the acceptor and can be defined as seen in equation (2). R_0 to the sixth power is therefore dependant upon the dipole - dipole orientation factor κ, the quantum yield of the donor ϕ_D, the refractive index of the medium n and the overlapping integral between donor emission and acceptor excitation spectra Γ. It is this overlap between spectra which is one of the defining conditions of a FRET setup, as it relates to the average rate of FRET k_{ET} and can be set by the use of a suitable donor acceptor pair to optimize the experiment.

While usually set between an acceptor and a donor of different kinds of fluophores, thus named hetero - FRET, a FRET event is also possible between two molecules of the same fluophore, then called a homo - FRET[24]. While conventional hetero - FRET setups are quantified with different methods such as photobleaching or via a change in the donor fluorescence lifetime[27], homo - FRET is usually examined by looking at changes in the anisotropy.

$$r = \frac{GI_{par} - I_{per}}{GI_{par} + 2I_{per}}$$ (3)

The anisotropy is calculated as seen in equation (3) and is dependant on the intensity of the parallel I_{par} and the perpendicular polarized light I_{per}, as well as the G-Factor G, which corrects for disparities in detection sensitivities in the experimental setup of the microscope.

During anisotropy measurements polarised light (e.g. a laser) is used to specifically excite fluophores with a similarly aligned dipole within the sample[28]. The emitted light is then divided according to the polarization. Perpendicular and parallel polarizations are either measured sequentially one after another or at the same time with two separate channels for detection. An objective with low numerical aperture (NA) is usually used for such experiments as it does not perturb the ratio of parallel to perpendicular polarized emitted light.

Changes in anisotropy mainly result from either the change of the dipole orientation due to rotational movement of the molecule or due to a FRET event. The former is of importance in the case of small molecules such as fluorescent dyes, while of no significant importance in larger molecules such as FPs

The G-factor of an experimental setup can be determined, when measuring a fluophore with a known anisotropy, ideally one with $r \approx 0$ (e.g. fluorescein) using equation (4).

$$G = \frac{I_{per}}{I_{par}} \qquad (4)$$

This is due to the fast rotational movement of a small molecule such as fluorescein, which effectively makes the orientation of the dipole parallel to the exciting light a mute point.

Of special interest within the potential applications in live cells was the use of homo-FRET to examine FP - tagged ApoER2 \ Vldlr dimerization \ oligomerization upon interaction with Reelin. A sufficient overlap integral between excitation and emission spectra for all FPs in question exist (Figure 1). Experiments were closely modelled to a similar successful approach, proofing the oligomerization of receptors upon binding of a ligand[29].

Anisotropy measurements in conjunction with photobleaching can even be used to examine the cluster size of the FP- tagged protein of interest[30]. When examining anisotropy in a time resolved manner, it is further possible to discern the ratio of fluorophores in clusters from those that exist in a monomeric form[31].

Fluorescent Proteins

Since the green fluorescent protein (GFP) was first established as a tool for the visualization of cellular processes[32,33] it has become one of the most widespread tools in microscopy applications[34,35].
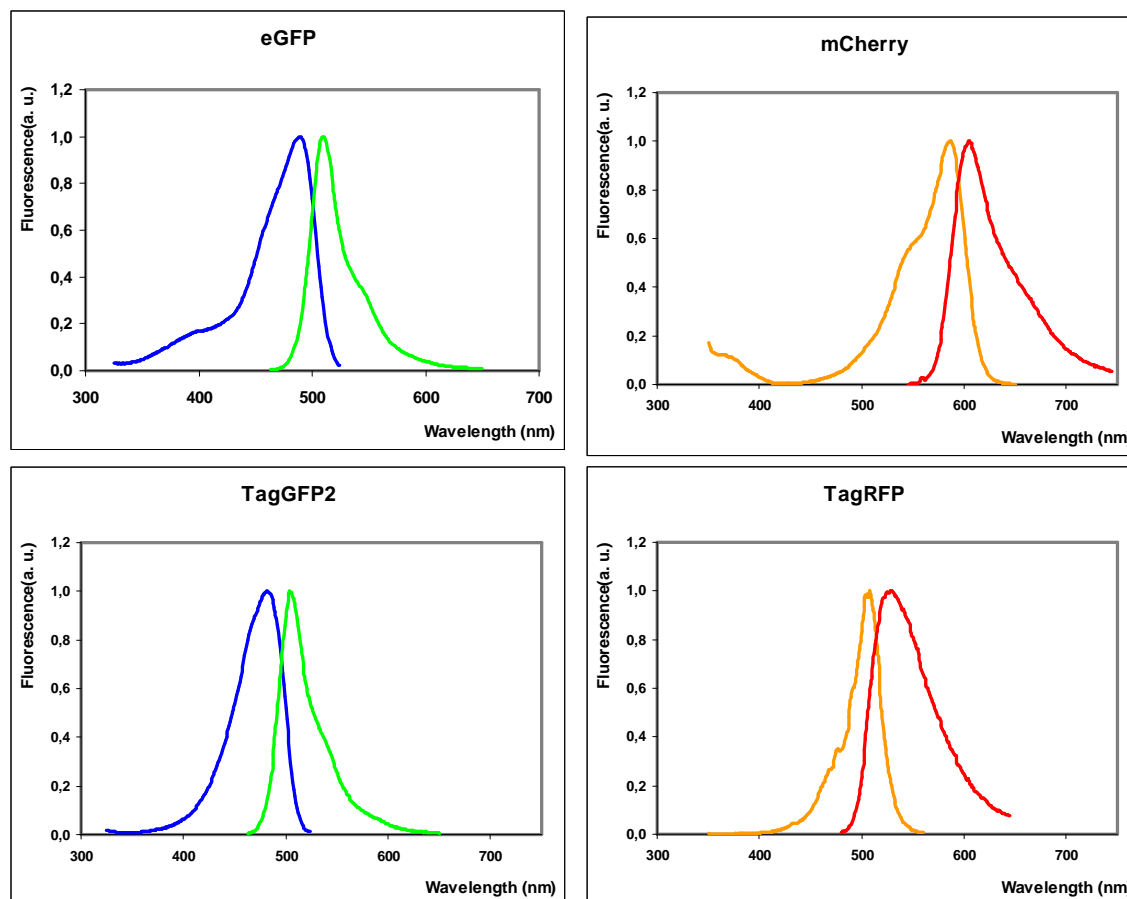

Figure 1: Fluorescent Protein Spectra. EGFP, TagGFP2 spectra are colored blue for excitation, green for emission, whereas mCherry and TagRFP are orange for excitation and red for emission. (Spectral information obtained either from Evrogen or Tsienlab)

Originally isolated from the *Aequorea victoria* jellyfish, wildtype GFP has been modified to make it more photostable, be brighter, have a better quantum yield and to be better suitable for expression in various model organisms and cultured cells. One such protein is the enhanced GFP (EGFP)[36]. Other modifications where aimed at broadening the colour palette and providing a monomeric fluorescent protein. The mFruit proteins (mCherry, mStrawberry , mOrange, e.g.), which were produced from mRFP[37] are examples for such engineered FPs [38].

Protein	Excitation Maximum (nm)	Emission Maximum (nm)	Extinction Coefficient (M^{-1} cm^{-1})	Quantum Yield	Relative brightness	Förster Distance of FRET pair (nm)
EGFP	489	509	55000	0.60	1.00	5.1
mCherry	587	610	72000	0.22	0.48	
TagGFP2	483	506	56500	0.61	1.05	5.7
TagRFP	555	584	100000	0.48	1.42	

Table 1: Summary of Fluorescent Protein Properties.

The daunting task of selecting suitable FPs for the task at hand Here two pairs of each one red and one green fluorescent protein, EGFP and mCherry, TagGFP2 and TagRFP, where selected as potential fusion protein tags (Table 1)[34,39,40]. In general FPs with a high relative brightness, which is dependant on the extinction coefficient (describes the likelihood of a fluophore absorbing a photon) and the quantum yield (number of emitted photons per photon used to excite) are preferable. Separate extinction and excitation spectra are also desirable when using two FPs in tandem(Figure 1). The EGFP, mCherry pair [41,42] as well as the TagGFP2, TagRFP pair have been shown to be applicable in hetero - FRET experiments[43].

While mCherry and EGFP exhibit broad excitation spectra, making them suitable as acceptors in a FRET experiment, TagGFP2 and TagRFP have much slimmer excitation and emission spectra, making them less prone to cross excitation and donor bleed through. However, either combination of one green (EGFP or TagGFP2) and one red (mCherry or TagRFP) fluorescent protein is a viable option for a hetero FRET setup.

GFP variants such as EGFP have also been used successfully in functional anisotropy imaging experiments[44], as has pTAGGFP[45] and mCherry. Besides established uses in FRET experiments, the mCherry, TagGFP2 and TagRFP were chosen because of the availability of their sequences in vectors sharing a common backbone, This facilitates easier cloning, as the receptor sequences could be removed from existing vectors (Figure 2) into vectors with a different FP - tag, with a simple double digestion (*SalI, HindIII*) and subsequent ligation (Figure 3).
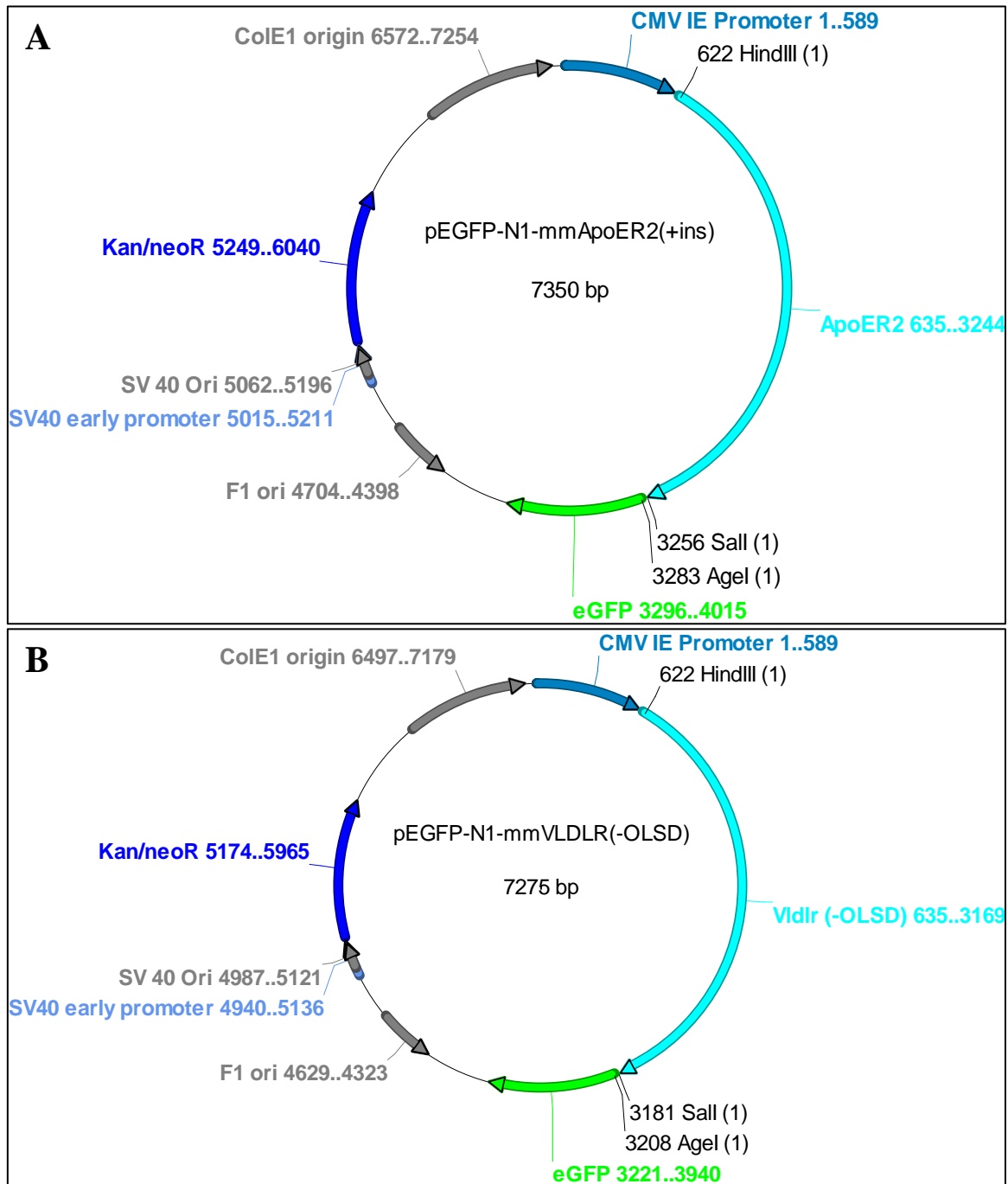
Figure 2: pEGFP-N1-Receptor plasmid maps. Map illustrating the composition of the pEGFP-N1 vector containing either anApoER2 (**A**) or Vldlr (**B**) insert. Labeled are the *E.coli* origin of replication, colE1, its mammalian counterpart the SV 40 origin, a single strand origin F1 ori, a kanamycin / neomycin resistance gene with a corresponding SV 40 early promoter for mammalian expression, the gene of interest with the EGFP - tag and its promoter, CMV IE and relevant restriction enzyme sites (*HindIII, SalI* and *AgeI*).
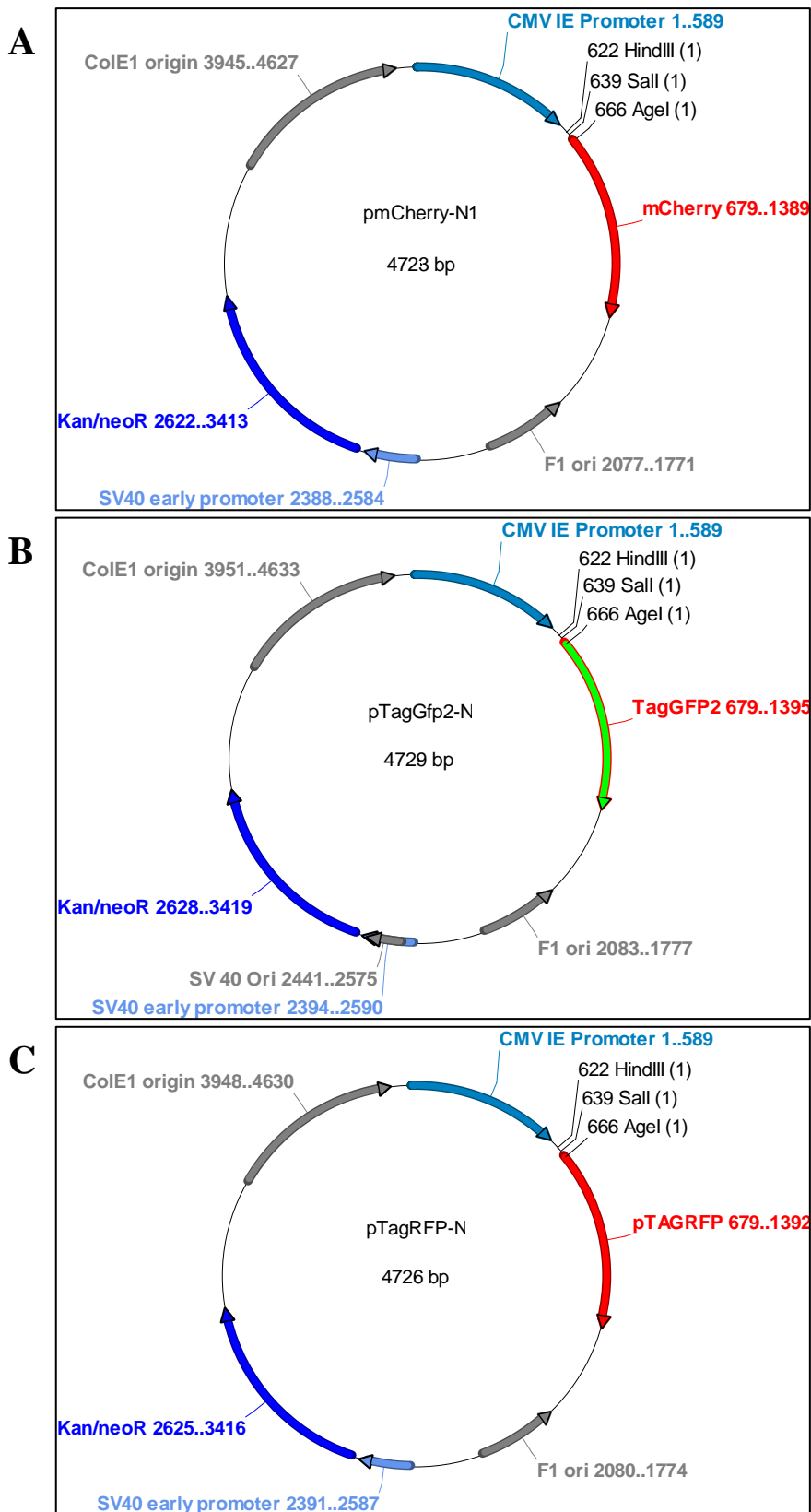
Figure 3: pmCherry-N1; pTagGFP2-N; pTagRFP-N plasmid maps. Labeled are the *E.coli* origin of replication, colE1, its mammalian counterpart the SV 40 origin, a single strand origin F1 ori, a kanamycin / neomycin resistance gene with a corresponding SV 40 early promoter for mammalian expression, fluorescent protein tag (mCherry **(A)**, TagGFP2 **(B)** or TagRFP**(C)**) and its promoter, CMV IE and relevant restriction enzyme sites (*HindIII, SalI* and *AgeI*).

Linker Separating Fluorescent Proteins from Receptors

One of the dilemmas of expressing fusion proteins is that a prediction of the interaction between the domains of the protein of interest and the tag cannot be made easily. The resulting folding of the hybrid - protein may easily interfere with the function of the protein of interest in different ways, most common problems being aggregation of the protein in clusters, inactive protein complexes and altered trafficking[46].

The multiple cloning site of in the vector backbones in question codes for a proline rich linker (RILQSTVPRARDPPVATM, Figure 4A), that may interfere with correct protein folding.

Different designs of linkers separating functional domains in fusion proteins have been described as efficacious in separating fluorescent proteins from each other[47,48]. Helical linkers with the strong helix motif (EAAAK) where shown to be effective in separating the fluorescent proteins while keeping their functionality intact, as where flexible linkers with a motive containing amino acids with shorter sidestrands (GSS).

To easily substitute the original proline rich linker with a linker of choice two restriction sites close to the end of the multiple cloning site were used. Oligonucleotides for the linkers were designed to have the correct overhangs for ligation with a *SalI, AgeI* double digested backbone (Figure 4). Furthermore helical linkers were designed with either 3 (RILQST EAAAK EAAAK EAAAK EAAA PVATM) or 5 (RILQST EAAAK EAAAK EAAAK EAAAK EAAAK EAAA PVATM) repetitions of the EAAAK motif (Figure 4B, D). For flexible linkers sequences with 6 (RILQST GSS GSS GSS GSS GSS GSS PVATM) or 10 (RILQST GSS GSS GSS GSS GSS GSS GSS GSS GSS GSS PVATM) repeats of GSS where used.

A   Original

```
R   I   L   Q   S   T   V   P   R   A   R   D   P   P   V   A   T   M
      cag tcg acg gta ccg cgg gcc cgg gat cca ccg gtc gcc acc atg
          SalI                                  AgeI
```

B   Helical Linker

```
                                        repeat n-times
R   I   L   Q   S   T   E   A   A   A  K   E   A   A   A  K   E   A   A
5'    cag tcg acc gag gcc gcc gcc aag gag gcc gca gcc aag gag gcc gcc
                   x   a   x   x   x   a   a   x   x   x   a   a   x   x
                   x   t   x   x   x   t   t   x   x   x   t   t   x   x
3'    gtc agc tgg ctc cgg cgg cgg ttc ctc cgg cgt cgg ttc ctc cgg cgg
SalI
```

```
 A   P   V   A   T   M
gca ccg gtc gcc acc atg   3'
  x
  x
cgt ggc cag cgg tgg tac   5'
    AgeI
```

C   Flexible Linker

```
              repeat n-times
R   I   L   Q   S   T   G   G   S   G   G   S   P   V   A   T   M
5'    cag tcg acc ggg ggg tcg ggg ggg tca ccg gtc gcc acc atg   3'
                  x   x   x   x   x   x   x
                  x   x   x   x   x   x   x
3'    gtc agc tgg ccc ccc agc ccc ccc agt ggc cag cgg tgg tac   5'
          SalI                              AgeI
```

D   Designs:

Small Helical Linker (SH; 21 aa, 63 bases)

```
5' tcg acc gag gcc gcc gcc aag gag gcc gca gcc aag gag gcc gca gcc aag
3'       gg ctc cgg cgg cgg ttc ctc cgg cgt cgg ttc ctc cgg cgt cgg ttc

gag gcc gcc gca        3'
ctc cgg cgg cgt ggc c 5'
```

Long Helical Linker (LH; 31 aa, 93 bases)

```
5' tcg acc gag gcc gcc gcc aag gag gcc gca gcc aag gag gcc gcg gcc aag
3'       gg ctc cgg cgg cgg ttc ctc cgg cgt cgg ttc ctc cgg cgc cgg ttc

gag gcc gca gcc aag gag gcc gca gcc aag gag gcc gcc gca        3'
ctc cgg cgt cgg ttc ctc cgg cgt cgg ttc ctc cgg cgg cgt ggc c 5'
```

Designs:

Small Flexible Linker (SH; 20 aa, 60 bases)

```
5' tcg acc ggt gga tct ggt gga tct ggt gga tct ggt gga tct ggt gga tct
3'       gg cca cct aga cca cct aga cca cct aga cca cct aga cca cct aga

ggt gga tca        3'
cca cct agt ggc c 5'
```

Long Flexible Linker (LF; 32 aa, 96 bases)

```
5' tcg acc ggt gga tct ggt gga tct ggt gga tct ggt gga tct ggt gga tct
3'       gg cca cct aga cca cct aga cca cct aga cca cct aga cca cct aga

ggt gga tct ggt gga tct ggt gga tct ggt gga tct ggt gga tca        3'
cca cct aga cca cct aga cca cct aga cca cct aga cca cct agt ggc c 5'
```

Figure 4: Linker Design. Amino acid sequences (single capital letters) and their corresponding base pair triplets (lower case letters) for the original linker sequence (**A**) and the general designs of helical (**B**) flexible linkers (**C**). Underlined sequences represent the restriction sites for *SalI* and *AgeI* used for cloning of the linker sequences. Middle lanes represent wobbles and potential alternatives of third base pairs in designed DNA sequences. Sequences of the designed linkers, with short and long variants for either helical or flexible designs are shown in (**D**).

Methods

Agarose Gel Electrophoresis (AGE)

Agarose gels were either prepared with 1% agarose for plasmid backbone and insert restrictions as well as for the determination of correct plasmid length in newly cloned colonies and 2% agarose for the control of linker - annealing in 1x TAE Buffer. They were run at 100 V with either $1.4 * 10^{-4}$ % ethidium bromide or 5 µl Midori Green™ per 100 ml of gel.

DNA Gel Extraction

DNA was extracted from agarose gels using the QIAquick Gel Extraction Kit^{TM} according to manual instructions. The restricted DNA fragments of expected length were excised using a fresh scalpel and weighed. Per mg of DNA containing gel 3µl of QG Buffer were added and the tubes were put at 55°C for 10', while being vortexed every two minutes. After 1µl of isopropanol per mg of gel was added, the solution was moved to a binding column, where it was allowed to sit for 2'. The column was then centrifuged at 10krpm in a table top centrifuge, the flowthrough was discarded. The column was washed twice with PE Buffer by centrifugation at 10 krpm for 2' and discarding of the flowthrough. After 2' of dry centrifugation at 10 krpm, DNA was eluted with 40 µl of ddH$_2$O. DNA concentration was determined using a Nanodrop 2000™ device.

Miniprep

For DNA minipreps the Wizard® Plus SV Minipreps DNA Purification System was used following manufacturer instructions. LB medium containing kanamycin (30µg/ml) for selection was inoculated with an *E. coli* colony and incubated at 37°C. The overnight culture was precipitated at 5000 x g, the resulting supernatant was discarded and the pellet resuspended in Resuspension Solution. After adding Lysis Solution and inverting the test tube 5 times, of Alkaline Protease Solution was added, upon which the test tube was inverted for a further 5 times. The lysis was allowed to proceed for 5', after which Neutralization Solution was added and mixed by inverting. Coagulated cell debris was precipitated by centrifugation at maximum speed for 10'. Thereafter the supernatant was transferred to the Spin Column and DNA bound to the column by centrifugation maximum speed for 1'. The column was then washed twice with the Column Wash Solution using the same centrifugation settings. After an additional dry centrifugation

16

step DNA was eluted with nuclease free water. DNA concentration was determined using a Nanodrop 2000™ device.

Midiprep

Midiprep plasmid purifications were made using the PureYield^{TM} Plasmid Midiprep System as described in the user manual. LB with kanamycin (30µg/ml) was inoculated with a bacterial stock and let grow overnight at 37°C. The bacterial culture was centrifuged for 15' at 5000xg, after which the supernatant was removed. The deposited cells were resuspended in Resuspension Solution and Lysis Solution was added. After gently mixing for about 20", Neutralization Solution was added. The resulting lysate was moved to a PureYield^{TM} Cleaning Column sitting above a PureYield^{TM} Binding and vacuum was applied until the Cleaning Column had run dry. The Cleaning Column was subsequently washed once with Endotoxin Removal Wash Solution, then with Column Was Solution through utilization of the vacuum. Plasmid DNA was then eluted with DNAse free water. DNA concentration was measured with a Nanodrop 2000™.

Cloning of Receptors

Vector backbones (pmCherry-N1 (Clontech), pTagGFP2-N (Evrogen), pTagRFP-N (Evrogen)) as well as plasmids containing the sequences of the receptors (pEGFP-N1-mmApoER2, pEGFP-N1-mmVldlr; pEGFP-N1(Clontech)) were double digested with *SalI* (ThermoScientific) and *HindIII* (ThermoScientific) in 2x Buffer Tango. Cut DNA was divided by fragment length using AGE (see above), then excised and purified (see above). Putative inserts (mmApoER2 and mmVldlr sequences) were ligated to backbones using T4 ligase (ThermoScientific) with a molar ratio of backbone to insert of 1 to 3. The ligation was then transformed into chemical competent *E.coli* Top10F using a heat shock method at 42°C for 30".

The transformed bacteria were plated on LB kanamycin (30µg/ml) plates and let grow overnight at 37°C. Colonies from these plates were used for inoculation of liquid LB kanamycin (30µg/ml). Minipreps as well as bacterial stocks (see above) were prepared from the o\n cultures. The plasmids were analyzed by linearization with a suitable restriction enzyme (*HindIII*) and subsequent AGE, then by sequencing through a postal service (LGC Genomics).

Plasmid maps were drawn using ApE-A plasmid editor (V. 2.0.45).

Annealing and Cloning of Oligonucleotides

Purchased oligonucleotides (Table 2) were annealed by heating to 95°C, and slowly cooling to 20°C over the timeframe of one hour using a thermocycler. To facilitate correct base pairing the oligonucleotides (10µM) annealing was performed with the following buffer: 10mM Tris (pH 7.5-8.0); 50 mM NaCl; 1mM EDTA.

Linker	Coding Strand Oligonucleotides (5' → 3')	Template Strand Oligonucleotide (5' → 3')
Short Helical (**SH**)	TCG ACC GAG GCC GCC GCC AAG GAG GCC GCA GCC AAG GAG GCC GCA GCC AAG GAG GCC GCC GCA	C CGG TGC GGC GGC CTC CTT GGC TGC GGC CTC CTT GGC TGC GGC CTC CTT GGC GGC GGC CTC GG
Long Helical (**LH**)	TCG ACC GAG GCC GCC GCC AAG GAG GCC GCA GCC AAG GAG GCC GCG GCC AAG GAG GCC GCA GCC AAG GAG GCC GCA GCC AAG GAG GCC GCC GCA	C CGG TGC GGC GGC CTC CTT GGC TGC GGC CTC CTT GGC TGC GGC CTC CTT GGC CGC GGC CTC CTT GGC TGC GGC CTC CTT GGC GGC GGC CTC GG
Short Flexible (**SF**)	TCG ACC GGT GGA TCT GGT GGA TCT GGT GGA TCT GGT GGA TCT GGT GGA TCT GGT GGA TCA	C CGG TGA TCC ACC AGA TCC ACC AGA TCC ACC AGA TCC ACC AGA TCC ACC AGA TCC ACC GG
Long Flexible (**LF**)	TCG ACC GGT GGA TCT GGT GGA TCT GGT GGA TCT GGT GGA TCT GGT GGA TCT GGT GGA TCT GGT GGA TCT GGT GGA TCA	C CGG TGA TCC ACC AGA TCC ACC AGA TCC ACC AGA TCC ACC AGA TCC ACC AGA TCC ACC AGA TCC ACC AGA TCC ACC GG

Table 2: Oligo Nucleotides for Annealing: Underlined areas show regions of overlap for ligation.

Vector backbones (pmCherry-N1, pTagGFP2-N, and pTagRFP-N) were digested with *SalI* (ThermoScientific) and *AgeI* (ThermoScientific). The digested backbones were purified by AGE and sequential Gel Extraction (see above). The ligation of the annealed oligonucleotides to the vector backbones were performed with a 600 times excess of oligonucleotides using T4 ligase (ThermoScientific). Further steps during the transformation were performed as described above (Cloning of Receptors). Correct plasmid sequence was check with digestion (*HindIII, BamH1*).

18

Bacterial Stocks

Bacterial stocks were prepared from fresh o\n cultures with a ratio of 85% culture to 15% sterile glycerol and immediately stored at -80°C.

Cell Cultivation

HEK 293 and NIH 3T3 cells were cultivated in Dulbecco's modified Eagle's Medium (DMEM, PAA\ GE Healthcare) supplemented with 10 % fetal calf serum (FCS, Invitrogen) as well as penicillin \ streptomycin (P\S, Invitrogen). HEK 293 cells with a stable expression of one of the receptor - fluorescent protein fusions (cell lines CA II, CA III, CV VI, GA III, GA IV, GV I, GV II, RA III, RA IV, RV I, RV II) were cultivated in h DMEM, 10% FCS, +P\S further supplemented with 0.5 mg/ml G418. 3T3 Dab, A(+) and V(-)[49] cell lines were cultivated in DMEM, 10% FCS, +P\S, 0.5 mg/ml puromycin. All cell lines were kept at 37°C with 7.5% CO^2. To detach cells from the cell culture dishes they were treated with trypsin.

Cell Extracts

Cell extracts from mammalian cell cultures were prepared with radioimmunoprecipitation assay (RIPA) buffer (10 mM sodium phosphate (pH 7.4), 150 mM NaCl, 2 mM EDTA, 50 mM NaF, 2 mM Na3VO4, 1% β-mercaptoethanol, 1% Triton X-100, 1% sodium deoxycholate, 0.1% SDS, completed with a protease inhibitor cocktail (Roche)) as a lysis buffer.

Dishes of cells with a density of 80 to 100 % were washed twice with ice cold PBS, then cells were scraped off the plates into a Ripa buffer suspension. The cell suspension were stored on ice for 15' then sonicated for 10" and kept on ice for further 15'. Cellular debris was then precipitated by centrifugation and the supernatant stored at -80°C. Protein concentrations were measured using the Pierce® BCA Protein Assay.

Transfection of Eukaryotic Cells

Transfections of NIH 3T3 and HEK 293 cells were performed with PeqFect DNA or Lipofectamine® 2000 according to the manufacturer specifications.

Cell extracts and confocal microscopy imaging were performed after 48 to 72 hours.

Cells in 60 mm cell culture dishes with a density of 70% were switched to an antibiotic free medium (DMEM, 10% FCS).

Lipofectamine 2000

Plasmid DNA (8µg) was added to Optimem® Reduced Serum Medium. Lipofectamine (20µl) was mixed with Optimem. After 5 minutes of incubation, the two fractions were combined and let to incubate for 20'. The DNA \ Lipofectamine mix was pipetted gently on the prepared cells. The medium was changed to DMEM (10% FCS, P\S) after 6 hours.

PeqFect DNA

Plasmid DNA (6µg), PeqFect DNA (12µl) were added to Optimem® Reduced Serum Medium and let to incubate for 15'. The transfection mixture was then gently dripped on the prepared cells. After 6 hours P\S was added to the DMEM Medium. Medium was switched 24 h after transfection.

Producing Stable Single Cell Lines

Selection to produce stable cell lines was started 48 hours after transfection by switching to DMEM (10% FCS, P\S, 1 mg/ml G418). To assure G418 efficacy an untransfected cell sample was treated with G418 as well. Medium was switched every 2 to 3 days thereafter to maintain stable G418 concentration. If necessary, cells were split to maintain a density of 40 to 80 %. Selection was continued until all cells of the untreated control were no longer viable (15 to 19 days after transfection). Upon which 120 cells were seeded into a 96 well chamber in order to produce single cell clones. The wells were checked 24 hours later and the number of cells within them was counted. Single clones were grown until a sufficient population was present, and then were examined with confocal microscopy as well as for correct protein expression.

Western Blot

Separating Gel	8%	10 %	Stacking Gel	4 %
H2O	2.3 ml	2.0 ml	H2O	1,4 ml
30 % Acrylamide Mix	1.3 ml	1.7 ml	30 % Acrylamide Mix	0,33 ml
1.5 M Tris (pH8,8)	1.3ml	1.3ml	1 M Tris (pH6,8)	0,25 ml
10% SDS	50 µl	50 µl	10% SDS	20 µl
10% APS	50 µl	50 µl	10% APS	20 µl
TEMED	3 µl	2 µl	TEMED	2 µl

Table 3: Composition of SDS-PAGE Gels.

Protein extracts were heated to 95°C with a reducing buffer to denaturize. SDS Page gels were prepared as described below (Table 3) and run at 30mA per Gel. Proteins were transferred to a Nitrocellulose Membrane with a wet blot system.

After blocking the membranes were bound overnight with the corresponding antibody (Table 4) at 4°C. Detection was performed by binding with an HRP-tagged secondary antibody (1:20000 dilution) and Super Signal West Pico Chemiluminescent Substrate.

Name	Antigen	Dilution	Host	Clonality	Blocking Solution	Supplier
a20[50]	mmApoER2 cytoplasmic tail	1 : 8000	rabbit	polyclonal	5% powdered milk in PBS-T	
a74[20]	mmVldlr 1st ligand binding repeat	1 : 20000	rabbit	polyclonal	5% powdered milk in PBS-T	
D4	Dab-1	1 : 8000	mouse	monoclonal	5% BSA in PBS-T	Andre Goffinet (University of Louvain, Brussels, Belgium)
1c51	mCherry	1: 1000	mouse	monoclonal	5% BSA in PBS-T	Novus Biologicals
Anti-Tag(CGY)FP	TagGFP2	1:8000	rabbit	polyclonal	5% BSA in PBS-T	Evrogen
Anti-tRFP	TagRFP	1:5000	rabbit	polyclonal	5% BSA in PBS-T	Evrogen

Table 4: Antibodies used for WB.

Dialysis of RCM \ MCM

Reelin conditioned medium (RCM)[2] and mock conditioned medium (MCM) were dialysed o\n against PBS to remove riboflavin, phenol red and other substances that possibly interfering with fluorescence microscopy.

Confocal Microscopy

Confocal microscopy pictures of live cells where taken with a Zeiss LSM 510 microscope with a 63x, 1.4 NA, oil objective using ZEN imaging software. Cells were pictured at RT with PBS 10mM Hepes as medium.

Green fluorescent proteins (EGFP, TagGFP2) were imaged employing a 488 nm argon laser for excitation passing a 98µm pinhole, and a 505nm long pass filter, resulting in pictures with a pixel size of 0.097 µm. Red fluorescent proteins (mCherry, TagRFP) were

imaged using a 543 nm helium - neon laser for excitation passing a 107µm pinhole, and a 560nm long pass filter, resulting in pictures with a pixel size of 0.106 µm. Pictures with both red and green fluorescent proteins were imaged with the settings for green fluorescent proteins, but the green signal was restricted to 505 - 543 nm output.

Homo - FRET

Homo - FRET experiments were performed using a Picoquant MicroTime 200 confocal microscope with a low NA objective (0.65NA, 60x, Air). For the excitation of TagGFP2 a 440 nm diode laser was used, fluorescence was curtailed with a 460nm long pass filter, passing a 75µm pinhole and then split with a polarizing beam splitter into perpendicular and parallel signals collected simultaneously with two individual detectors. The laser power used ranged from 8 to 60µW. Pixel size was set to 0.097µm.

Upon each application laser polarization was determined using a mirror and no bandpass filter. The G-factor (G) was measured as well using 10µM fluorescein.

GA IV and GV I cells were cultivated on ibiTreat µ-Slides (Ibidi) for microscopy.

Cells were washed with PBS and incubated for 20' at 4°C with MCM or RCM dialysed against PBS, supplemented with 10mMHepes or with PBS, 10mMHepes containing antibodies recognizing the receptors ligand binding domain (Table 5). An anti Reelin antibody (a83) was used as a control, with the dilution used in the corresponding experiment: 1:1000 dilution of a83 used with GA IV cells when compared to a186 and a 1:800 when used with GV I cells and compared to a187.

Name	Antigen	Dilution	Host	Clonality
a186[21]	mmApoER 2 ligand binding domain	1 : 1000	rabbit	polyclonal
a187[21]	mmVldlr ligand binding domain	1 : 800	rabbit	polyclonal
a83	Reelin	1 : 800 / 1:1000	rabbit	polyclonal

Table 5: Antibodies used for HomoFRET.

Microscopy was performed at RT, for no longer than 1h. Symphotime64 was used as the software for the interpretation of measured anisotropy data.

Results

EGFP - Receptor Fusions

Pre-existing pEGFP-N1 vectors with inserts of murine ApoER2 and Vldlr (Figure 2) were first used to attempt to determine the extract intracellular localization of the receptors. NIH 3T3 were used as a host for the FP - tagged receptors as it has been demonstrated to be a cell line suitable for examining the Reelin pathway[49]. On the other hand HEK 293 cells are well established for their high levels of protein expression, and thusly were used as a target cell line for transfection as well. The transfected cells were then imaged with confocal microscopy and the localization of the receptor was examined.

Transfected HE 293 cells were observed to have a high presence of the FP- tagged receptors in the cytoplasmic membrane (Figure 5, 293 eGA, 293 eGV). However a strong tendency for the aggregation of FP – tagged ApoER2 or Vldlr (bright dots) was also detectable. Such aggregations of fluorescent proteins are ill suited, if one wishes to use the cells in question for sensitive microscopy imaging. Experiments where the FP needs to be bleached (e.g. hetero FRET with donor bleaching) are especially hampered.

Upon transfection NIH 3T3 cells showed little to no localization of the FP – tagged receptors on the plasma membrane (Figure 5, 3T3 eGA, 3T3 eGV). As a sufficiently high presence of the FP-tagged receptors in the cell membrane was the key requirement for most further experiments neither of the 3T3 transfections were deemed suitable.
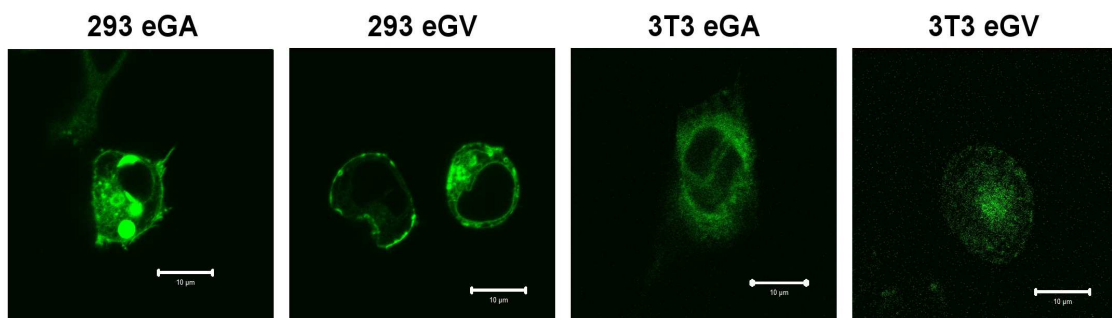

Figure 5: Confocal Microscopy of HEK 293 and 3T3 pEGFP-N1-mmApoER2 and pEGFP-N1-mmVldlr Transfections. HEK 293 and NIH 3T3 were transfected with either pEGFP-N1-mmApoER2 (293 eGA or 3T3 eGA) or pEGFP-N1-mmVldlr (293 eGV or 3T3 eGV) plasmids and observed with a LSM 510 confocal microscope. Bar size 10µm.

In conclusion, as neither combination of EGFP-N1- tagged receptors could be expressed in an applicable way in either HEK 293 or NIH 3T3 cells, different FPs were employed as tags.

mCherry - , TagGFP2 - , TagRFP - Receptor Fusions

The utilized expression vectors (pEGFP-N1; pmCherry-N1, pTagGFP2-N, pTagRFP-N) all share a common backbone as well as almost identical multiple cloning sites (MCS). Therefore obtaining the receptor sequences from the pre existing plasmids pEGFP-N1-ApoER2(+ins) and pEGFP-N1-mmVldlr (-OLSD) could be achieved by a simple double digestion with *SalI* and *HindIII* followed by ligation into the new vector backbones.
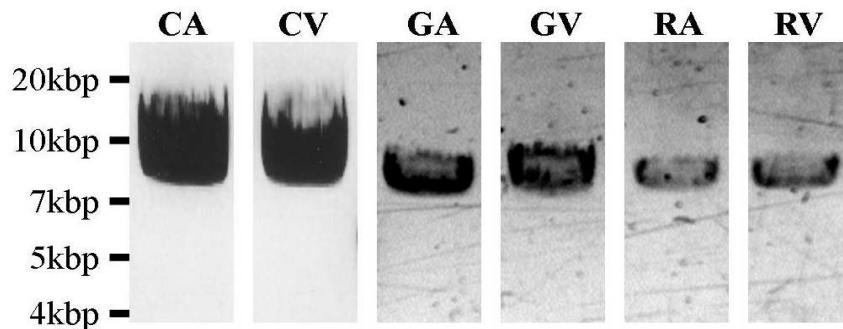

Figure 6: AGE of pmCherry-N1-\pTagGFP2-N-\pTagRFP-N- mmApoER2 \ mmVldlr *HindIII* digestions. Linearized vectors pmCherry-N1-mmApoER2 (CA), pmCherry-N1-Vldlr(CV), pTagGFP2-N-mmApoER2 (GA), pTagGFP2-N-Vldlr (GV), pTagRFP-N-mmApoER2 (RA) and pTagRFP-N-Vldlr (RV) showed bands at approximately 7.3 kb in a 1% agarose gel.

The results of this are vectors with a length of about 7.3 kb (Figure 6). Further to checking the length of the cloned vector DNA, the inserts were verified by sequencing.

The successfully cloned plasmids were then transfected into NIH 3T3 cells and examined with confocal microscopy (Figure 7). Transfections with pmCherry-N1-mmApoER2 (CA) and pmCherry-N1-mmVldlr (CV) showed poor localization to the cytoplasmic membrane, as fluorescence was mostly located in small amassments, possibly small aggregates or parts of the endomembrane system. Similarly pTagRFP-N-mmApoER2 (RA) and pTagRFP-N- mmVldlr (RV) show a defuse fluorescence mostly located to the cytoplasm. However pTagGFP2-N-mmApoER2 (GA) and pTagGFP2-N- mmVldlr (GV) manifested mostly in the cytoplasmic membrane and areas resembling ER and vesicles. The selection for stable cell lines was finished with NIH 3T3 cells transfected with CA, CV and GA plasmids, but except for CA no single clones were produced as imaging showed no particularly promising candidates.
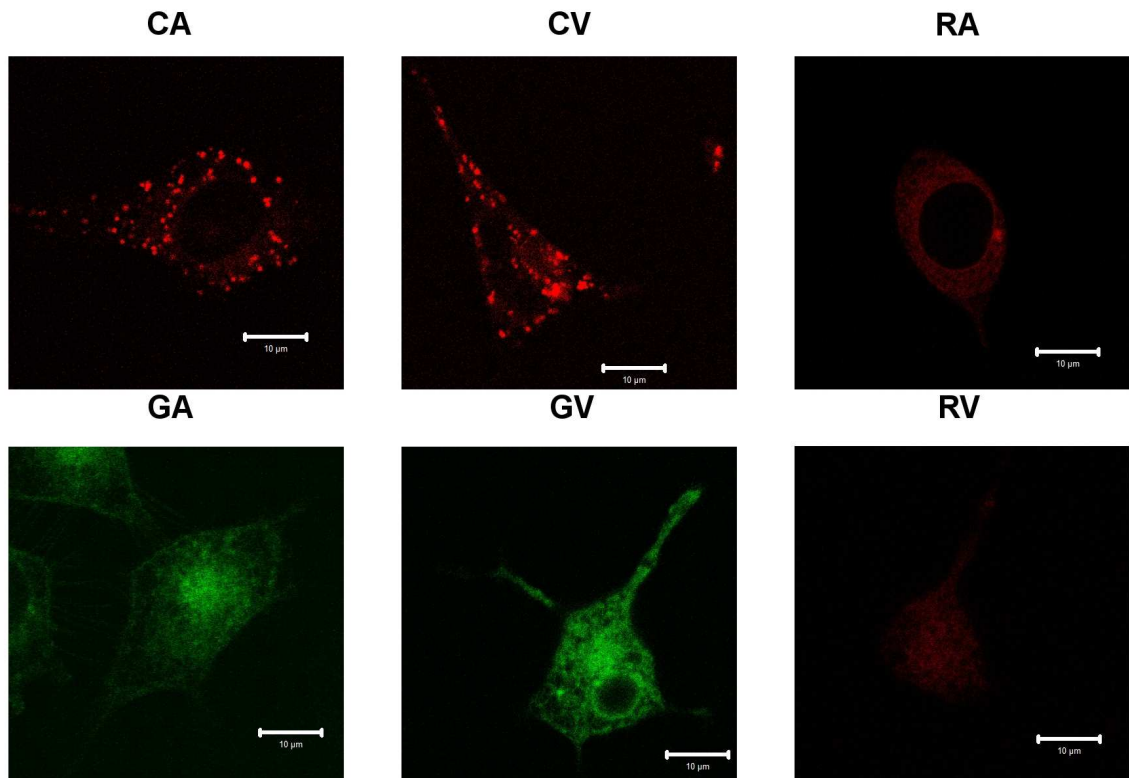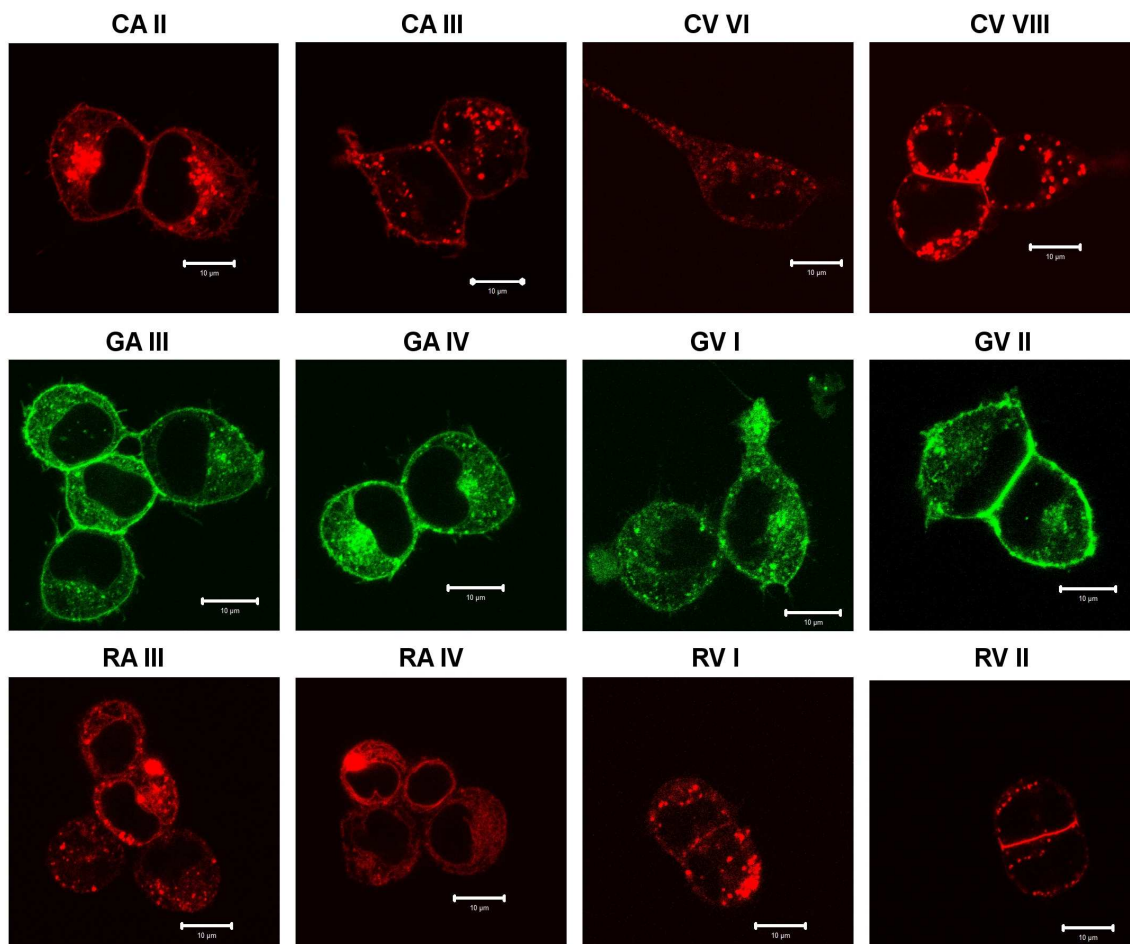
**Figure 7: Confocal Microscopy of 3T3 pmCherry-N1-\pTagGFP2-N-\pTagRFP-N- mmApoER2 \
mmVldlr Transfections. .** NIH 3T3 were transfected with pmCherry-N1-mmApoER2 (CA),
pmCherry-N1-Vldlr(CV), pTagGFP2-N-mmApoER2 (GA), pTagGFP2-N-Vldlr (GV), pTagRFP-N-
mmApoER2 (RA) or pTagRFP-N-Vldlr (RV) plasmids and observed with a LSM 510 confocal
microscope. Bar size 10µm.

Transfections of Hek 293 cells with the FP- tagged receptors showed better results than
those of NIH 3T3 cells. Hence stable cell lines grown from single cells were produced
from these transfections (Table 6).

Name	Plasmid used for Transfection	Derived From Cell Line	Clonality
CA II	pmCherry-N1-mmApoER2	Hek 293	single clone
CA III	pmCherry-N1-mmApoER2	Hek 293	single clone
CV VI	pmCherry-N1-mmVldlr	Hek 293	single clone
CV VIII	pmCherry-N1-mmVldlr	Hek 293	single clone
GA III	pTAGGFP2-N-mmApoER2	Hek 293	single clone
GA IV	pTAGGFP2-N-mmApoER2	Hek 293	single clone
GV I	pTAGGFP2-N-mmVldlr	Hek 293	single clone
GV II	pTAGGFP2-N-mmVldlr	Hek 293	single clone

Table 6: Stable Cell Lines Containing FP- Tagged ApoER2 \ Vldlr.

When imaged with a confocal microscope(Figure 8), cell lines CA II and CA III showed a strong presence of the ApoER2 - mCherry fusion protein in the plasma membrane but also some bright aggregations containing the fusion protein, possibly resulting from overburdened endomembrane system due to massive protein production. Comparable images were taken from cell lines CV VI and CVIII, with the latter having a much higher amount of mCherry - Vldlr in the cell membrane. In contrast cell lines produced with the pTagRFP-N backbone, RA III, RA IV, RV I and RV II were prone to accumulation of FP-fusion protein within the cytoplasm but showed very little in the plasma membrane. Furthermore, cell line RV II ceased proliferating shortly after the images below were taken and before it could be examined with a western blot.

Figure 8: Confocal Microscopy of HEK 293 pmCherry-N1-\pTagGFP2-N-\pTagRFP-N-mmApoER2 \ mmVldlr Single Clones. Hek 293 were transfected with pmCherry-N1-mmApoER2 (CA), pmCherry-N1-Vldlr(CV), pTagGFP2-N-mmApoER2 (GA III, GA IV), pTagGFP2-N-Vldlr (GV I, GV II), pTagRFP-N-mmApoER2 (RA III, RA IV) or pTagRFP-N-Vldlr (RV I, RV II) plasmids and then made into stable cell lines. Cells were imaged with a LSM 510 confocal microscope. Bar size 10µm.

These results are well mirrored in the western blot experiment made with extracts from the single clones (Figure 9). CA II and CA III cells were found to exhibit the double bands characteristic for ApoER2 that result from differential glycosylation (bands at 160, 200 kDa respectively), as well as some unspecific bands, when detected by the anti - ApoER2 antibody a20. Bands of the same lengths were detected with1c51, an antibody directed against the mCherry part of the fusion protein. The comparative size of 160 kDa and 200 kDa is somewhat more than expected, which would be 130 kDa and 160 kDa but aligns well enough with the double band of the untagged ApoER2 receptor, whose bands were detected at ~ 120 kDa and 150kDa.

CV VI and CV VIII exhibited bands at ~ 140 kDa, when using either a74 or 1c51 for detection. However some unspecific bands or products of degradation could be observed at ~ 120 kDa as well.

GA III and GAIV cell extracts showed distinct bands at ~ 160, 200 kDa and the least background of all the ApoER2 constructs when detecting with a20, and very concrete bands upon detection with antiTag(CGY).

GV I and GV II similarly showed rather concise bands at ~ 140kDa, when detected with either a74 or antiTag(CGY). Nonetheless, unspecific bands or a degradation products of Vldlr can be seen as a smear at ~ 100kDa.

RA III and RA IV showed a distinct third band at ~ 140kDa in addition to the bands at ~ 160, 200 kDa, possibly a product of specific degradation, as it could only be observed with the a20 antibody but not with anti-tRFP.

RV I shows similar band patterns as RA III with at least three different bands detected by a74 (140 kDa, 125 kDa and 110kDa) but only two by anti-tRFP (140 kDa and 125 kDa).
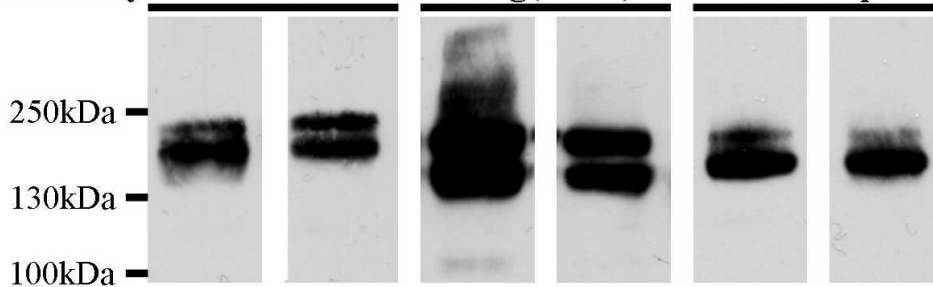
In conclusion Hek 293 derived cell lines GA IV and GV I were established as the primary tools for following assays, with CA III and CV VIII cell lines as backups in the red fluorescent spectrum.
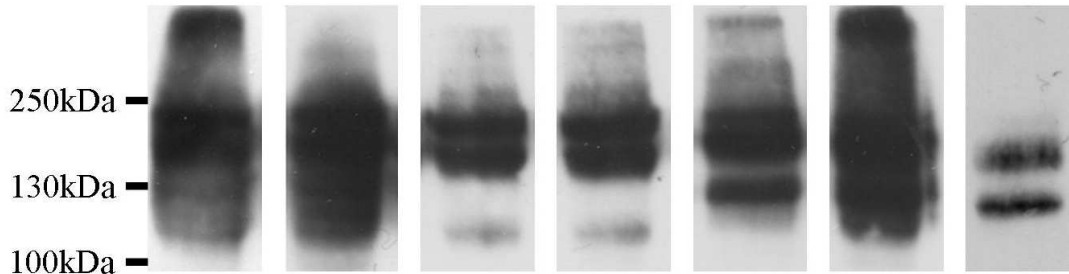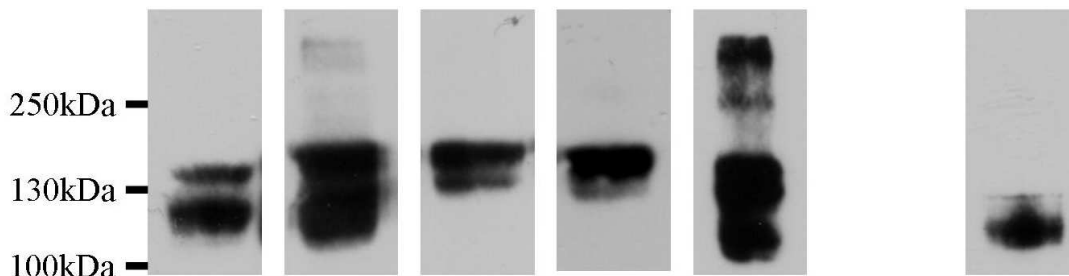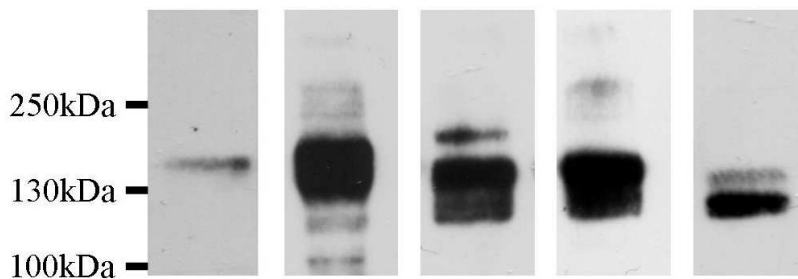
Figure 9: HEK 293 pmCherry-N1-\pTagGFP2-N-\pTagRFP-N- mmApoER2 \ mmVldlr Single Clone Western Blots. Protein extracts were detected with both an antibody recognizing the receptor part (a20 for ApoER2, a74 for Vldlr) and an antibody detecting the FP (1c51 for mCherry, antiTag(CGY)FP for TagGFP2 and anti-tRFP for TagRFP). Protein extracts (10µg) from HEK 293 single clones CA II, CA III, CV III, CV VIII, GA III, GA IV, GV I, GV II, RA III, RA IV and RV I were used. 3T3 A and V cell extracts (10µg) were used as positive controls for ApoER2 and Vldlr.

Linker Separating Fluorescent Proteins from Receptors

The exchange of the native linker sequence present in the backbone of pTagGFP2 and pTagRFP for different varieties of linker sequences was carried out with annealed oligonucleotides.

After the annealing process the oligonucleotides were examined with a high percentage agarose gel (Figure 10). As there was hardly any difference in the band patterns of annealed or unannealed oligonucleotides, it was concluded that the annealing process had not been very efficient.

Linker sequences where thus used in excess in relation to the *SalI, AgeI* digested vector backbone (600:1) to assure that a correct ligation can take place, even with a low percentage of correctly annealed linker DNA. Ligation of linker to linker was not an issue as all linker DNA was ordered without a 5' phosphate group. It is also possible that unnanealed oligonucleotide was ligated into the backbone[51], with one of the overlaps for the restriction site generating a correct orientation. The so obtained ligations where then used for transformations as described above.

The resulting plasmids where then analysed with *BamHI* and *HindIII* digestions. The expected result was for plasmids with a linker insert to be cut by *HindIII* ,but not by *BamHI* as its restriction site was part of the multiple cloning site, that was replaced by the new linker (Figure 10 B). This was indeed successfully done with all potential linker - plasmid combinations: pTAGGFP2-N with short helical linker (GSH), long helical linker (GLH), short flexible linker (GSF) or long flexible linker (GLF) as well as pTagRFP with a short helical linker (RSH), long helical linker (RLH), short flexible linker (RSF) or long flexible linker (RLF). Sequencing revealed that no clones with a correct sequence of the long flexible linker (GLF, RLF) could be successfully produced, most likely due to either mismatched basepairing during oligonucleotide annealing.

The remaining six new backbones with interspersed linker sequences were then digested with *SalI* and *HindIII*, ligated to the similarly restricted receptor sequences and used for transformations. The such established 12 distinct possible combinations of linker backbones with receptors ApoER2 (A) or Vldlr (V) were thus dubbed GSH A, GSH V, GLH A, GLH V, GSF A, GSF V, RSH A, RSH V, RLH A, RLH V, RSF A and RSF V.

They were examined for their correct length (~7.3kb; Figure 10 C), as well as checked by sequencing.
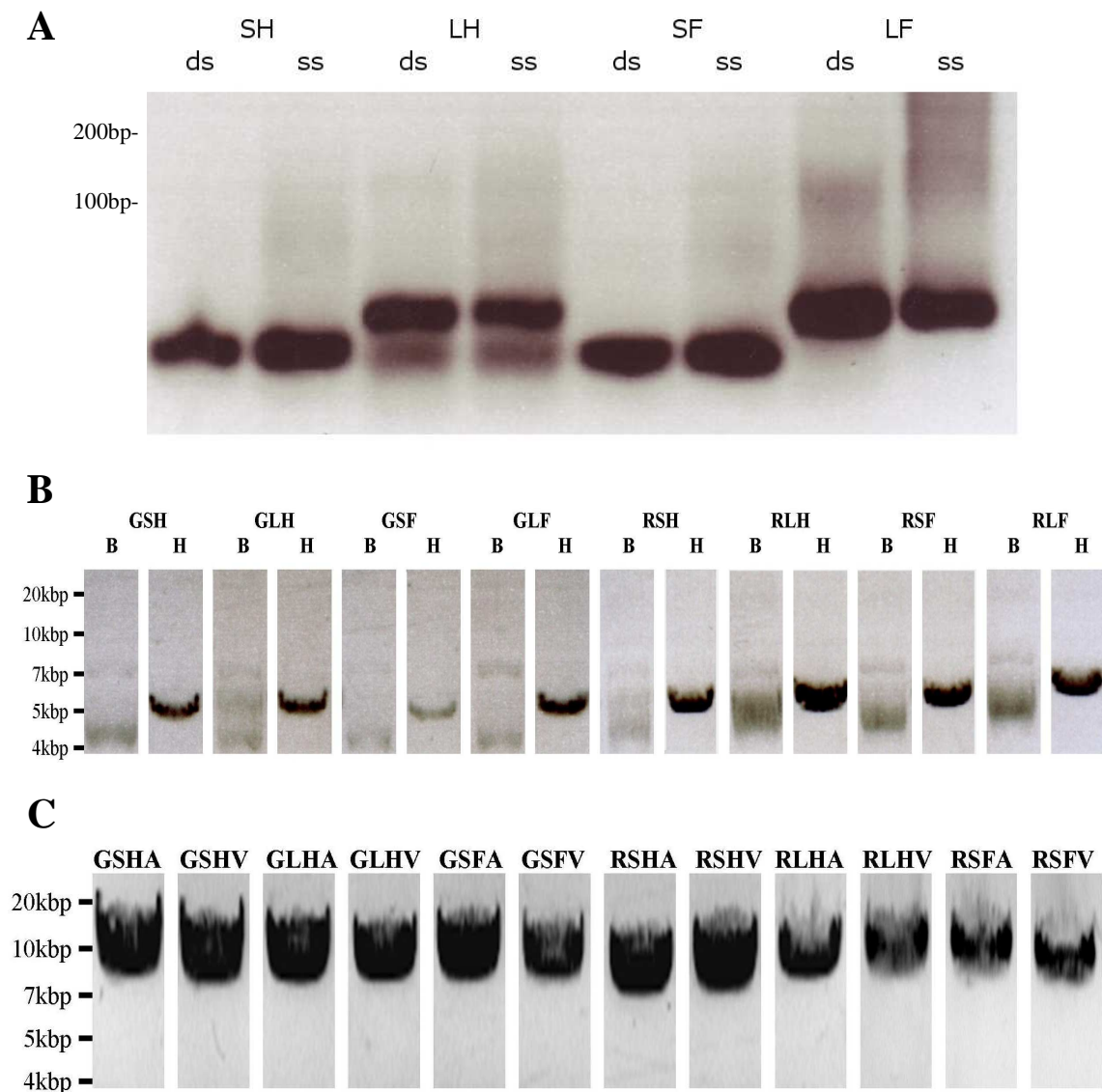
Figure 10: AGEs of pTagGFP2-N-\pTagRFP-N- linker - mmApoER2 \ mmVldlr. Mixture of coding and template strands of oligonucleotides small helical (SH), long helical (LH), small flexible (SF) and long flexible (LF) linkers before (ss) and after annealing (ds) were separated on a 2% agarose gel(**A**). Linearized vectors pTagGFP2-N \ pTagRFP-N containing linkers (GSH, GLH, GSF, GLF, RSH, RLH, RSF and RLF) exhibited bands at approximately 4.9 kb, on a 1% agarose gel. when digested with *HindIII* (H) but remain circular after *BamHI*(B)digestion (**B**). *HindIII* digestions of backbones with linker and receptor inserts (GSH A, GLH A, GSF A, RSH A, RLH A, RSF A GSH V, GLH V, GSF V, RSH V, RLH V and RSF V) showed a single band at approximately 7.3kb when separated on a 1% agarose gel.

The sequencing showed that clones from all twelve examined types of plasmids (GSH A, GLH A, GSF A, RSH A, RLH A, RSF A GSH V, GLH V, GSF V, RSH V, RLH V and RSF V) exhibited the correct sequence for their respective receptor insert.Then the newly obtained combinations of FP-tagged receptors were utilized via transfections to image their localization within NIH 3T3 and Hek 293 cells.
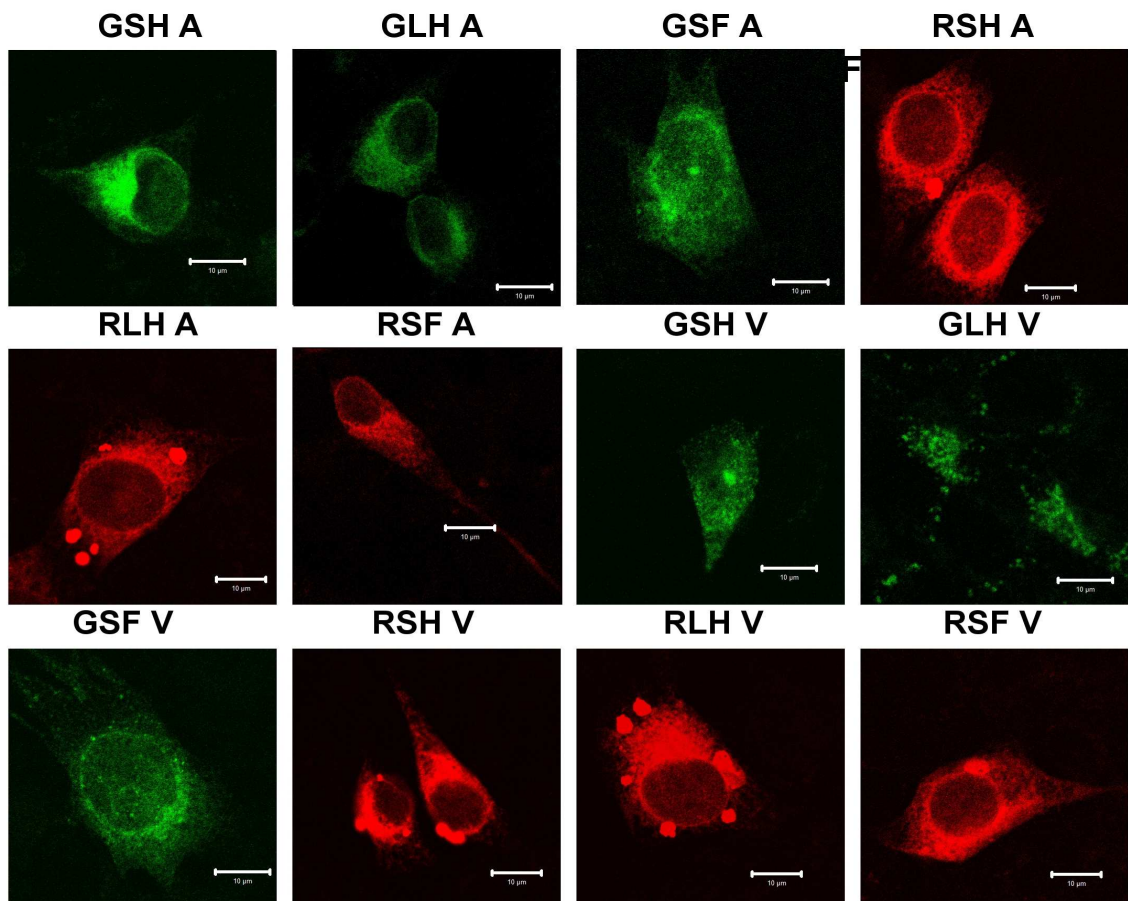
Figure 11: Confocal Microscopy of 3T3 pTagGFP2-N-linker \pTagRFP-N-linker - mmApoER2 \ mmVldlr Transfections. NIH 3T3 were transfected with GSH A, GLH A, GSF A, RSH A, RLH A, RSF A GSH V, GLH V, GSF V, RSH V, RLH V and RSF V plasmids and observed with a LSM 510 confocal microscope. Bar size 10µm.

Transfections of NIH 3T3 cells with the linker and receptor containing pTagGFP2-N \ pTagRFP-N plasmids as a whole resulted in cells with very little fluorescence detectable in the membrane (Figure 11). Furthermore transfections that involved a plasmid with a helical linker (e.g. RLH A, GSH V) had even more problems with accumulation of fluorescent proteins within the cell, than those containing the native proline rich linker sequence.

Hek 293 cells transfected with pTagGFP2-N or pTagRFP-N backbones containing the linker as well as a receptor, showed similar problems as their NIH 3T3 counterparts (Figure 12). While transfections with GSH A and GLH A resulted in cells with a very high amount of ApoER2-TagGFP2 fusion proteins in the membrane, they also exhibited large aggregations of the fusion proteins. In contrast transfections with GSH V and GLH V showed only weak aggregations with an average amount of fluorescently tagged proteins located in the membrane.
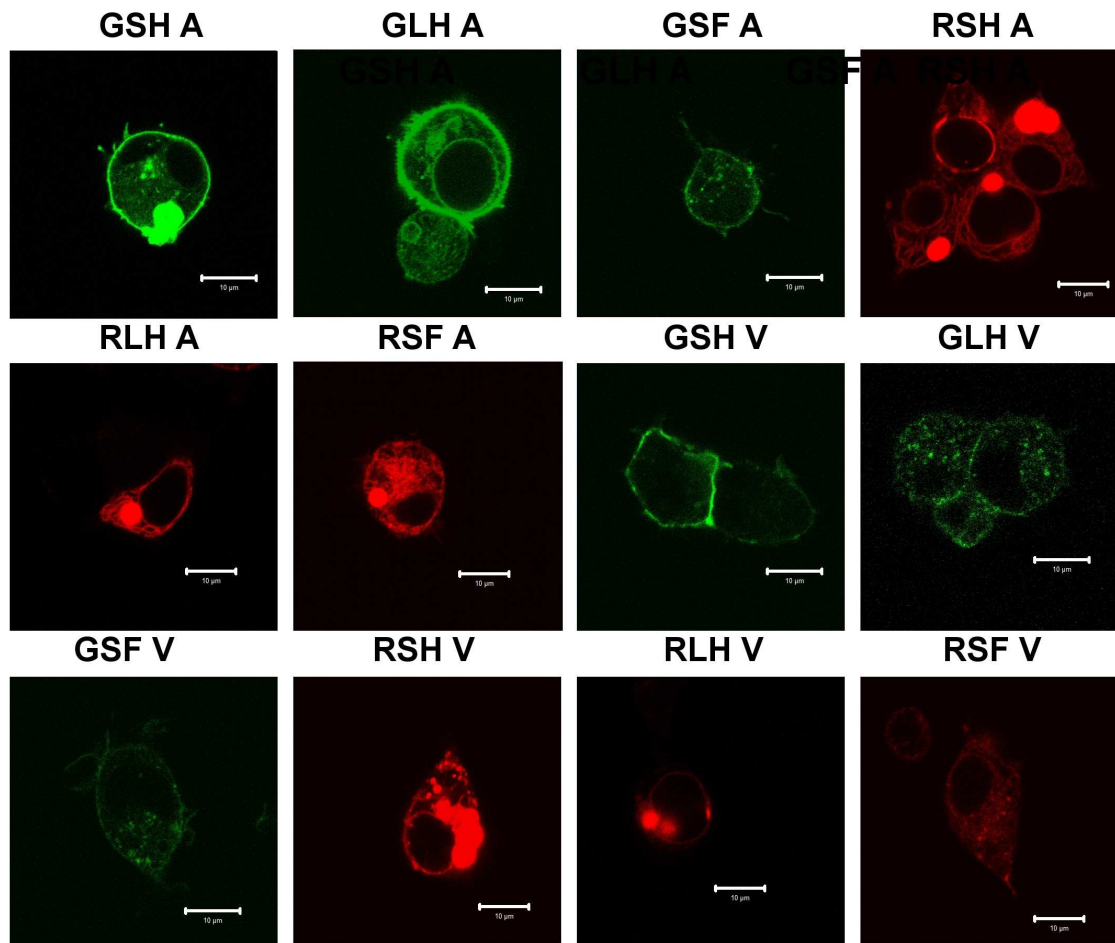
Figure 12: HEK 293 pTagGFP2-N-linker \pTagRFP-N-linker - mmApoER2 \ mmVldlr Transfections. Hek 293 cells were transfected with GSH A, GLH A, GSF A, RSH A, RLH A, RSF A GSH V, GLH V, GSF V, RSH V, RLH V and RSF V plasmids and observed with a LSM 510 confocal microscope. Bar size 10µm.

Hek 293 cells expressing the constructs from plasmids RSH A, RLH A, RSF A, RSH V and RSH V were shown to be especially likely to produce massive aggregations of fluorescently tagged receptors. Moreover RSF V transfections featured no specific localization of the FP - tagged Vldlr, with most of the visible fluorescence being in the cytoplasm.

Among the plasmids with modified linker sequences, GSF A and GSF V demonstrated the best localizations, as most of the fluorescence was located in the membrane, with no visible aggregates of FP.
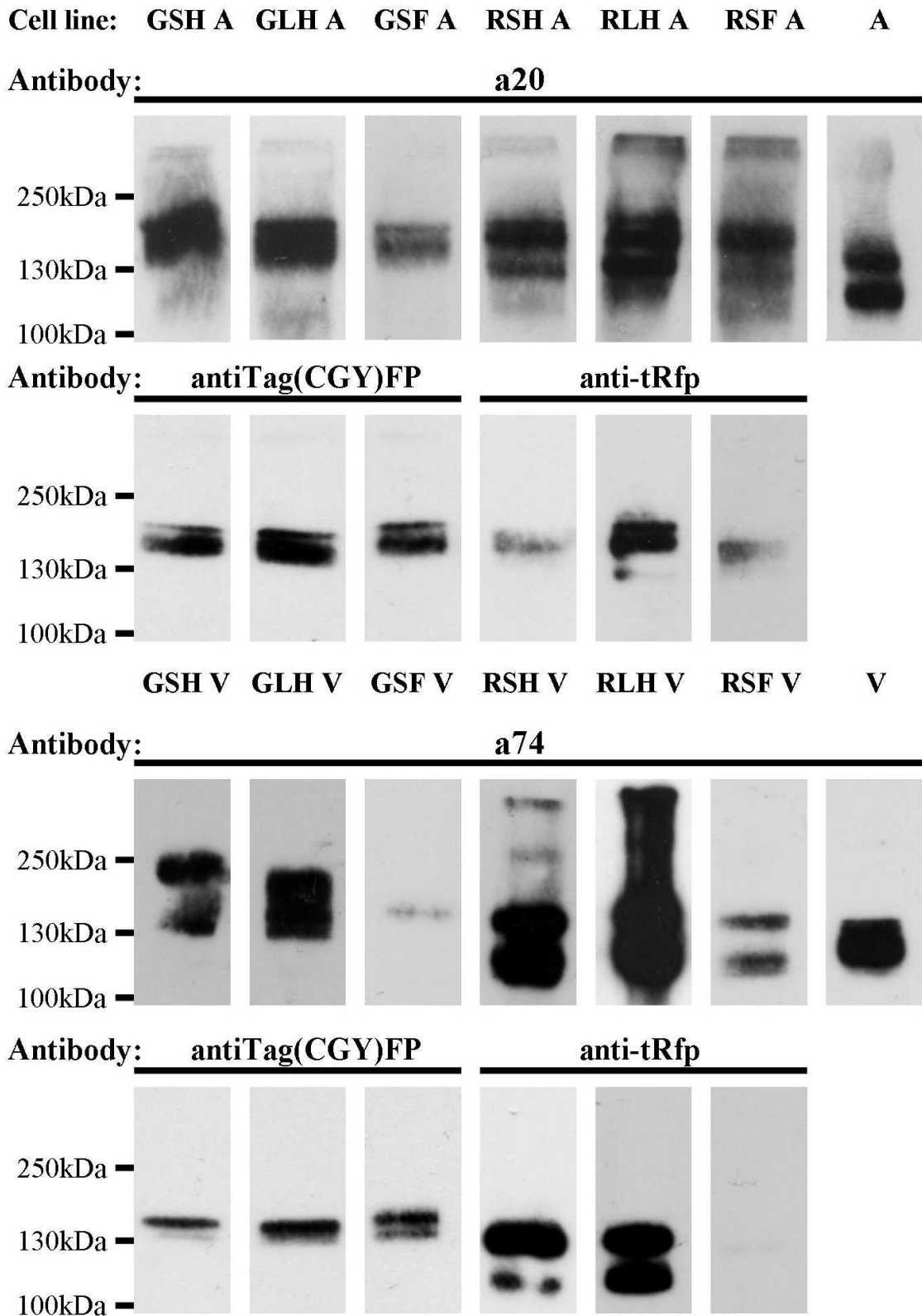
32

Figure 13: HEK 293 pTagGFP2-N-linker \ pTagRFP-N-linker - mmApoER2 \ mmVldlr Transfections Western Blots. Protein extracts were detected with both an antibody recognizing the receptor part (a20 for ApoER2, a74 for Vldlr) and an antibody detecting the FP (antiTag(CGY)FP for TagGFP2 and anti-tRFP for TagRFP). Protein extracts (1,5µg) from HEK 293 cells transfected with plasmids GSH A, GLH A, GSF A, RSH A, RLH A, RSF A GSH V, GLH V, GSF V, RSH V, RLH V and RSF V were used. 3T3 A and V cell extracts (3µg) were used as positive controls for ApoER2 and Vldlr.

This correlates well with the results from the western blot made with Hek 293 cell extracts (Figure 13). While almost all samples exhibit bands at the expected sizes, but for the GSF A and GSF V samples, they also exhibit strong backgrounds of unspecific nature or additional bands when detecting with the antibodies a20 or a74. In addition the TagRFP- Vldlr - fusion protein from RSF V transfected cells cannot be detected with the anti-tRfp antibody.

In summary only the plasmids containing the small flexible linker (GSF A and GSF V) have been shown to be a possible alternative to their native counterparts. However as by that time stable cell lines GA IV and GV I were established, further work with GSF A and GSF V was put on a hold.

Expression of both FP- tagged ApoER2 and Vldlr

Combinations of differently tagged ApoER2 and Vldlr were expressed jointly in the same cells to establish, whether both fluorescently tagged receptors can be expressed in the same cell without interfering with each other. This was done by transfecting existing stable cell lines with the other receptor tagged with a different FP. Thus GA IV cells were transfected with CV, GV I cells with CA, CA III cells with GV and CV VIII cells with GA plasmids.

The resulting cells were then imaged with a confocal microscope (Figure 14). As can be seen in all four combinations, shuttling of the fluorescently tagged receptors to the cell membrane was not perturbed and no excess increase in aggregation of FPs could be observed.

This is further confirmed by the analysis of the cell extracts with a western blot. Cell extracts of all four cell lines show expression that is similar to those of stable cell lines (Figure 9).

Out of the different combinations CV VIII transfected with GA plasmids did produce the best images, as localization to the membrane was high, while protein and fluorescence levels of the two fusion proteins appeared in the same range.
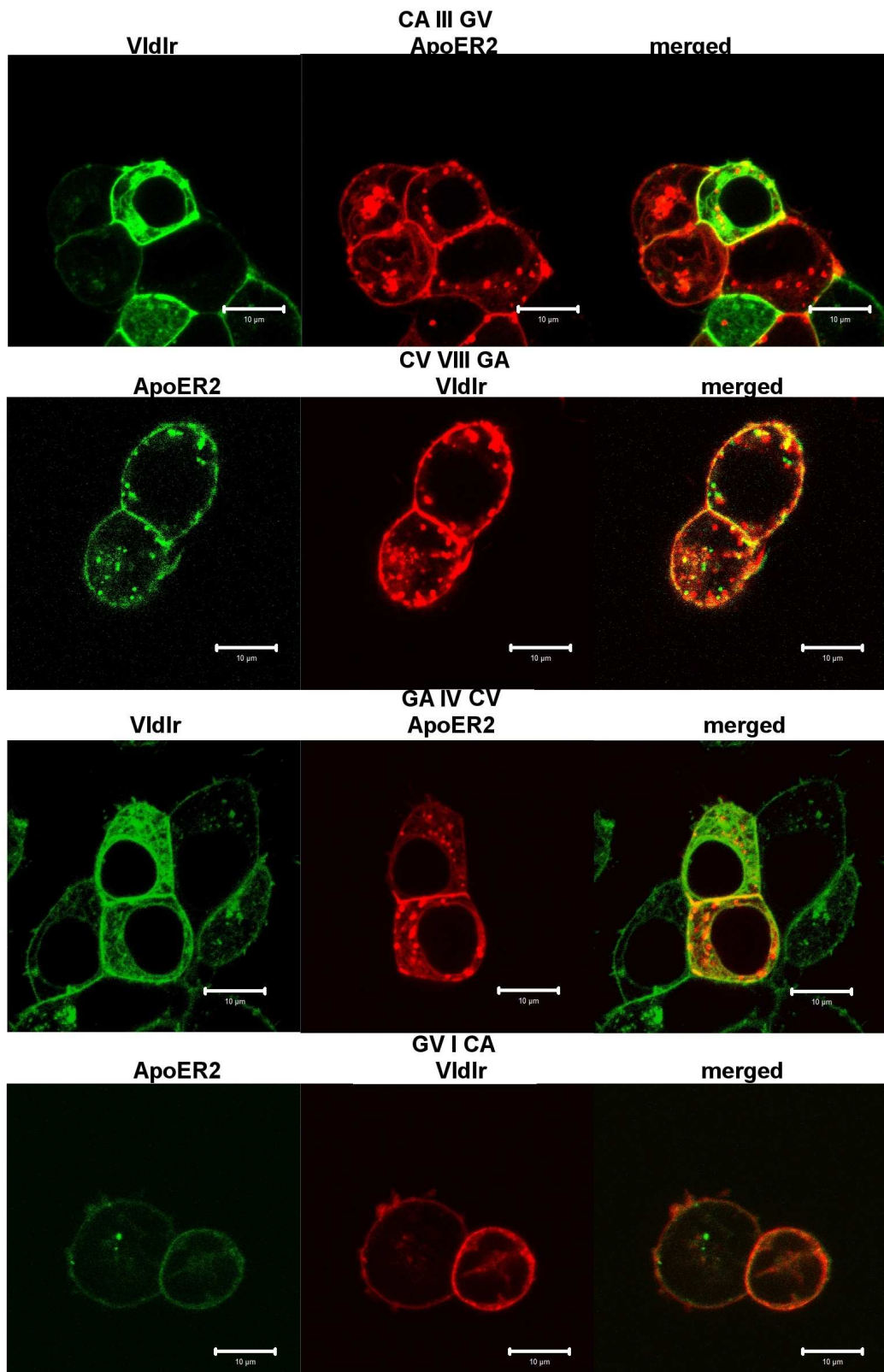
Figure 14: Confocal Microscopy of HEK 293 pmCherry-N1- \ pTagGFP2-N- - mmApoER2 \ mmVldlr Cotransfections. CA III, CV VIII, GA IV and GV I were transfected with CA, CV, GA and GV plasmids and observed with a LSM 510 confocal microscope. Bar size 10µm.

Cell line: CA III   CV VIII   GA IV   GV I

Transf.: GV   Ø   GA   Ø   CV   Ø   CA   Ø

Antibody: a20

250kDa —
130kDa —
100kDa —

Antibody: 1c51   antiTag(CGY)FP   1c51

250kDa —
130kDa —
100kDa —

Antibody: a74

250kDa —
130kDa —
100kDa —

Antibody: antiTag(CGY)FP   1c51   antiTag(CGY)FP
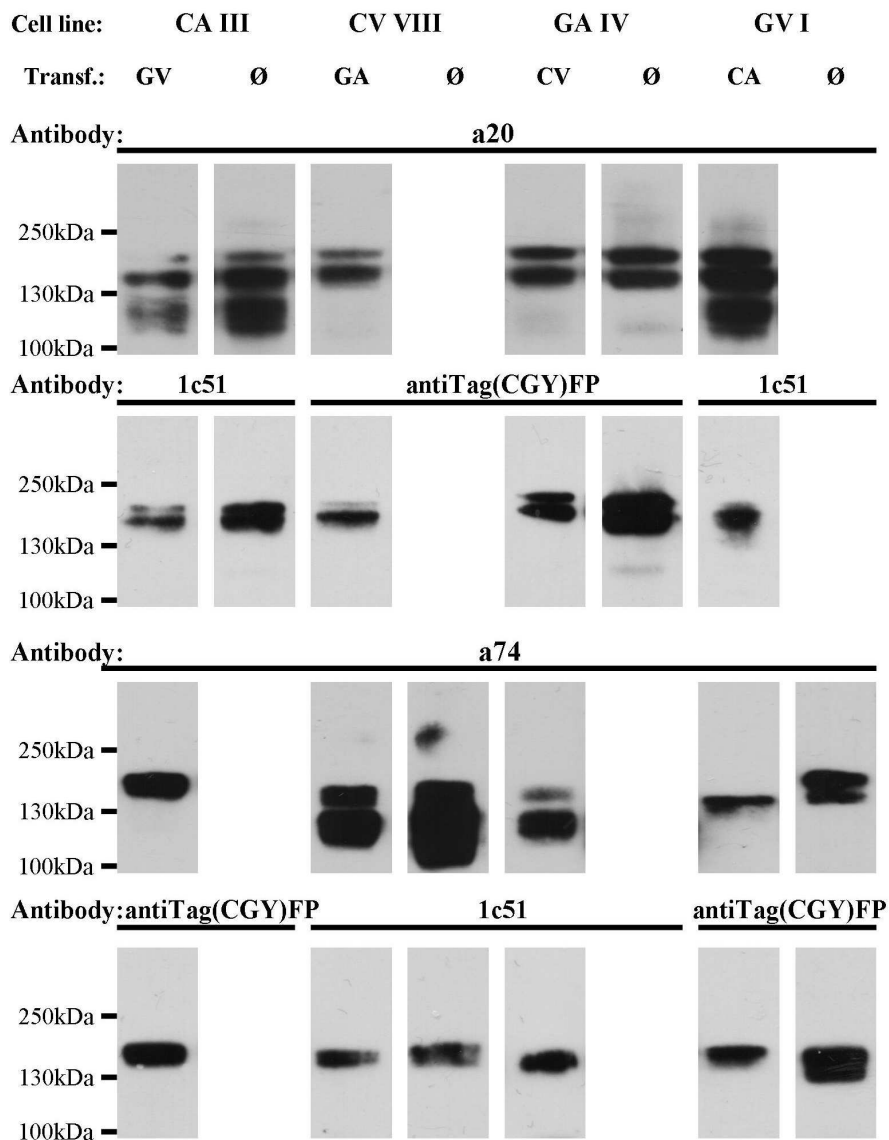
250kDa —
130kDa —
100kDa —

Figure 15: HEK 293 pmCherry-N1- \ pTagGFP2-N- mmApoER2 \ mmVldlr Cotransfections Western Blots. Protein extracts were detected with both an antibody recognizing the receptor part (a20 for ApoER2, a74 for Vldlr) and an antibody detecting the FP (1c51 for mCherry, antiTag(CGY)FP for TagGFP2 and anti-tRFP for TagRFP). Protein extracts ($2\mu g$) from HEK 293 single clones CA III, CV VIII, GA IV and GV I transfected with plasmids CA, CV, GA and GV were used.

Dab-1 - TagRFP

To study the potential interaction and relative position within cells of Dab1 in conjunction with either ApoER2 or Vldlr, GA IV and GV I cells were transfected with pTagRFP-N-mmDab1 (RD; generously provided by Sandra Gallista). Cells were then imaged with a confocal microscope (Figure 16).
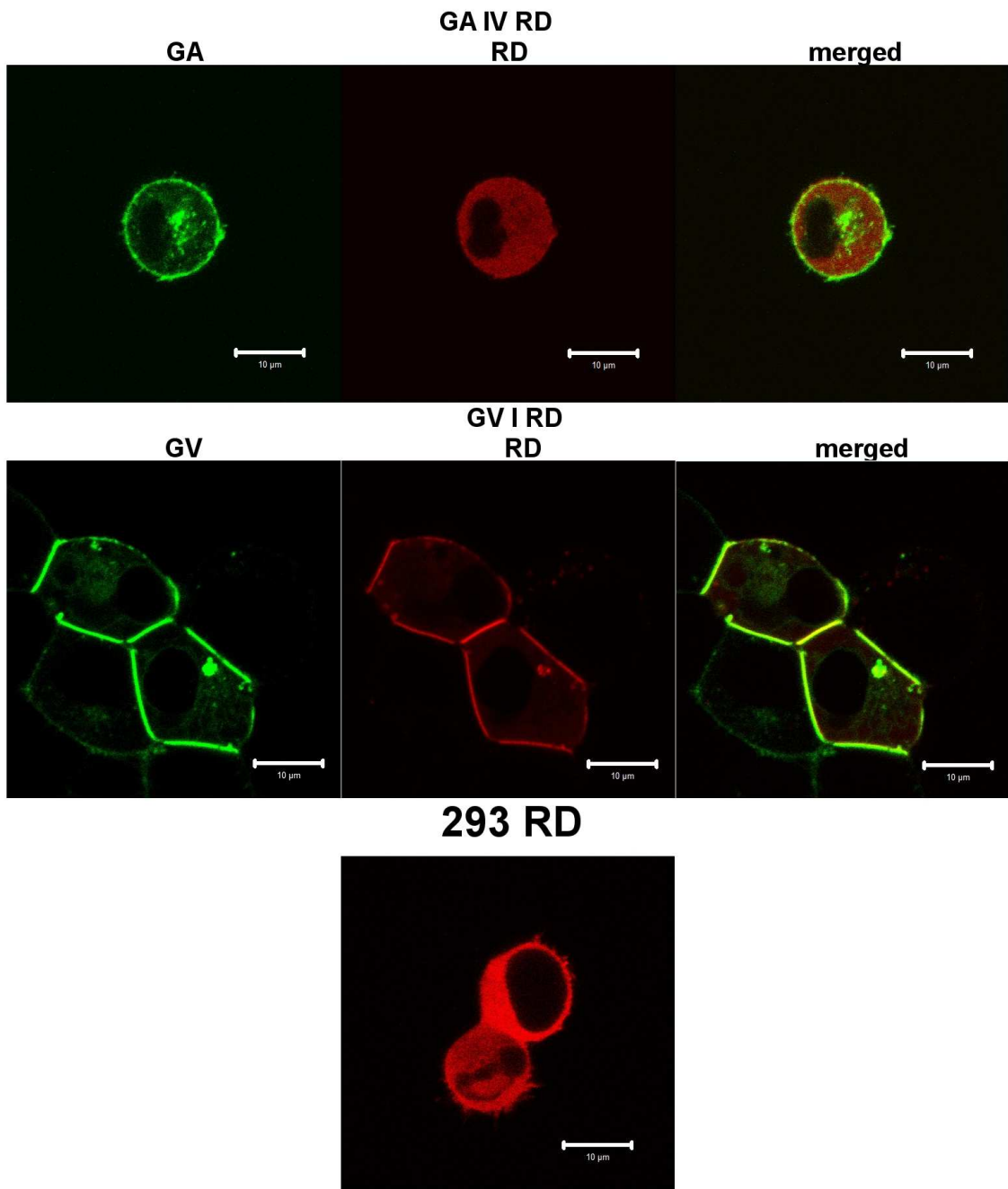
Figure 16: Confocal Microscopy of HEK 293 pTagGFP2-N- - mmApoER2 \ mmVldlr and pTagRFP-N-Dab1 Cotransfections. HEK 293, GA IV and GV I cells were transfected with pTagRFP-N-mmDab1 (RD) plasmid DNA and analyzed with a LSM 510 confocal microscope. Bar size 10µm.

Dab1 does not seem to colocalize with ApoER2 very strongly, without the presence of a ligand such as Reelin, and was shown to behave similar to cells without a known binding receptor (Hek 293). In contrast Dab1 is visible close to the plasma membrane and thus close to Vldlr if they are both expressed within the same cell.

Expression of the FP tagged receptors and Dab1 was also examined with a western blot (Figure 17). As can be seen expression of the TagRFP-N- Dab1 fusion protein did not

interfere with the expression of neither TagGFP2-N-mmApoER2 nor TagGFP2-N-mmVldlr expression. In extracts from cells expressing TagRFP-N- Dab1 fusion protein, multiple bands are visible, when trying to detect the TagRFP-N- Dab1 fusion protein, with both D4 as well as anti-tRFP antibodies. The origin of these additional bands is not clear but could be resulting from degradation of Dab1.
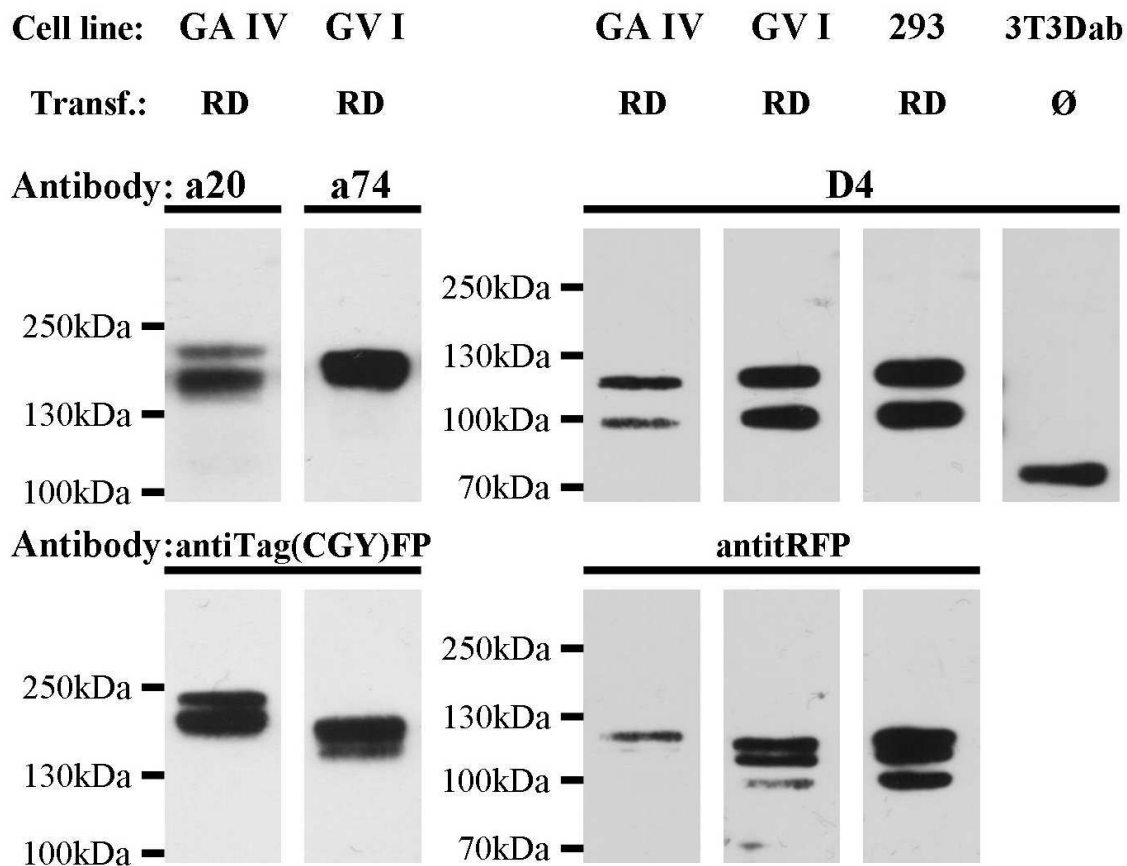

Figure 17: pTagGFP2-N- - mmApoER2 \ mmVldlr and pTagRFP-N-Dab1 Cotransfections Western Blots. Protein extracts were detected with both an antibody recognizing the PoI part (a20 for ApoER2, a74 for Vldlr, D4 for Dab1) and an antibody detecting the FP (antiTag(CGY)FP for TagGFP2 and anti-tRFP for TagRFP). Protein extracts (2µg) from HEK 293 single clones GA IV and GV I transfected with plasmid pTagRFP-N-mmDab1 (RD) were used. 3T3 Dab1 cell extract (4µg) was used as positive controls for Dab1.

Anisotropy Imaging

Anisotropy imaging was used to examine possible dimerization or oligomerization processes of the FP - tagged receptors induced by signal inducing ligands.

For these experiments GA IV and GV I cells were incubated with potential binding partners of their respective receptors (dialysed RCM, a186 used with GA IV cells, a187 used with GV I cells) or suitable control substances (dialysed RCM, a83 which binds to the intracellular domain of the receptor), then imaged with an anisotropy imaging setup.

The G-Factor was measured as well, which usually ranged from 0.97 to 0.98 and used to modify anisotropy calculations.

In the confocal microscopy images differences in anisotropy are very hard to discern (Figure 18, Figure 19). Possibly in the case of GA IV cells stimulated with dialysed Reelin conditioned medium alone, a slight difference in anisotropy can be detected when compared to the control experiment stimulated with dialysed mock conditioned medium.

Because the observed changes in anisotropy are very small the signals derived from cytoplasmic membranes of ten cells per each experimental group were combined and the absolute anisotropy of each pixel gathered. The resulting information was plotted within a graph (Figure 20).

There one can discern that there is indeed a shift in average anisotropy from 0.329 (MCM) to 0.321 in the case of GA IV cells when stimulated with Reelin. When GA IV cells were stimulated with an antibody (a186) known to bind to ApoER2 and induce Dab1 phosphorylation, a186, a similar shift to 0.321 in average anisotropy can be observed, with the control antibody producing an average anisotropy of 0.329 as well (Figure 20 A). These shifts are likely the result of homo - FRET events.

As the homo - FRET effects measured are very small and anisotropy decrease is correlated with the number of fluorescent proteins in a cluster, dimerization of ApoER2 seems likely to be the case. Other reasons for the small effect are that, as Reelin is internalized, and live cells were studied, the whole setup is in a constant flux reducing the amount of clustered receptors at a given time point.

No such shifts in anisotropy are discernable in the case of the Vldlr containing GV I cells (Figure 20 B). Indeed average anisotropies were measured at 0.325, 0.325, 0.323 and 0.327 for cells challenged with dialysed MCM, dialysed RCM, a83 and a187 respectively. In conclusion no homo - FRET events could be discerned in GV I cells under the set conditions.

While fundamental problems in the experimental setup are a possible cause, Vldlr and its faster speed of internalization[20] could also account for the lack in shift in anisotropy, in the case of the GV I cells. It has been shown by Duit et al. that, after binding Reelin at 4°C, cells expressing Vldlr quickly internalize Reelin, when moved back to 37°C. They showed that after only 10 minutes more than half of the Reelin is internalized. Contrarily

after the same amount of time more then 90% of the receptor bound Reelin still remains on the surface of cells with ApoER2 expression.

Potential changes in anisotropy within the endosomes can also not be documented, as it is not possible to discern them from other vesicles possibly travelling towards the cytoplasmic membrane.
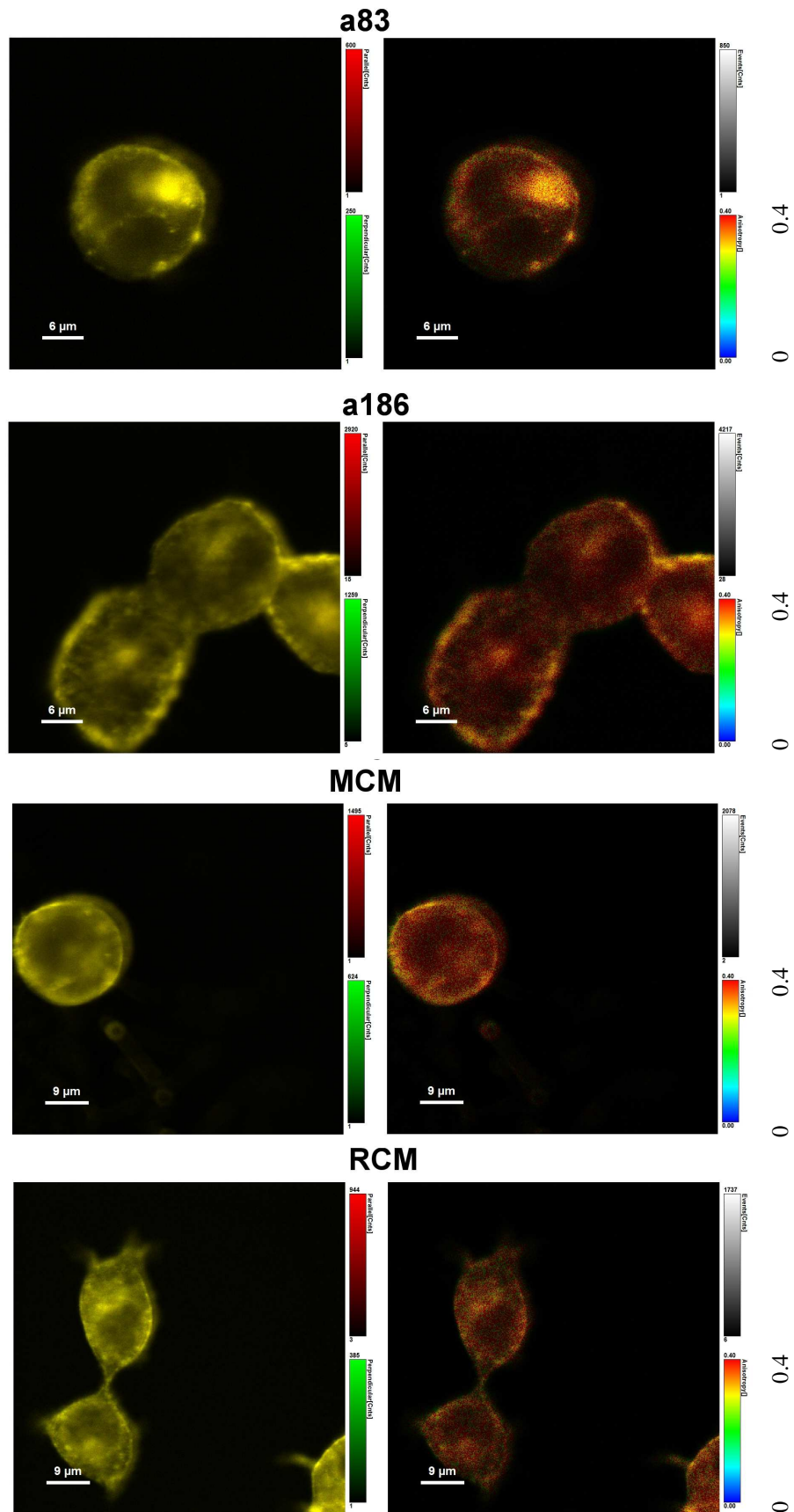
Figure 18: Confocal Microscopy and Anisotropy Imaging of GA IV cells. GA IV cells were stimulated with a binding partners to ApoER2 (a186, RCM) and suitable controls (a83, MCM). After 20' of stimulation at 4° cells were imaged according to their absolute fluorescence intensity (left) and their anisotropy (right). Scale bars show 6µm (top four images) and 9µm (bottom 4 images).
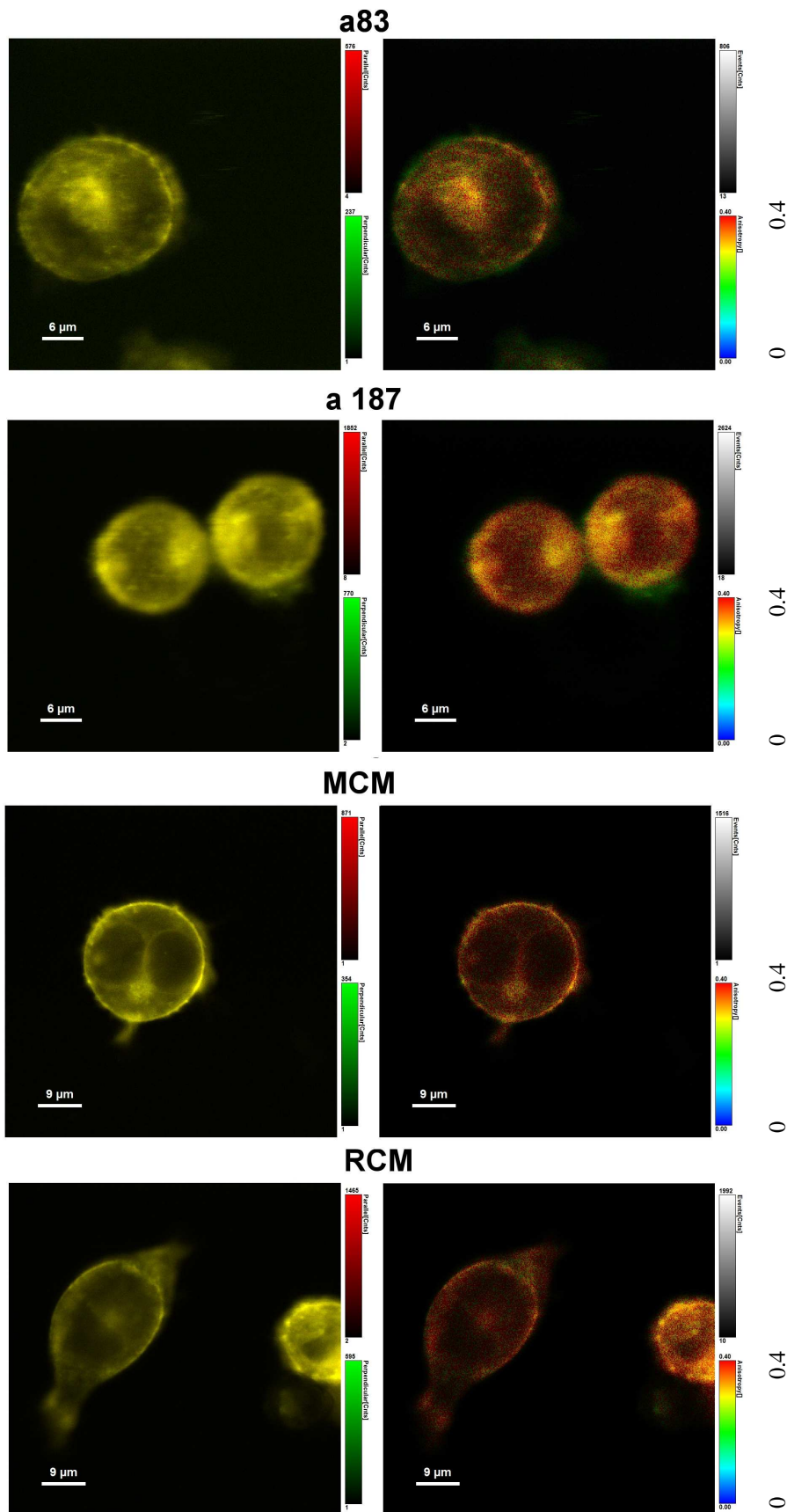
Figure 19: Confocal Microscopy and Anisotropy Imaging of GV I cells. GV I cells were stimulated with a binding partners to Vldlr (a187, RCM) and suitable controls (a83, MCM). After 20' of stimulation at 4° cells were imaged according to their absolute fluorescence intensity (left) and their anisotropy (right). Scale bars show 6µm (top four images) and 9µm (bottom 4 images).
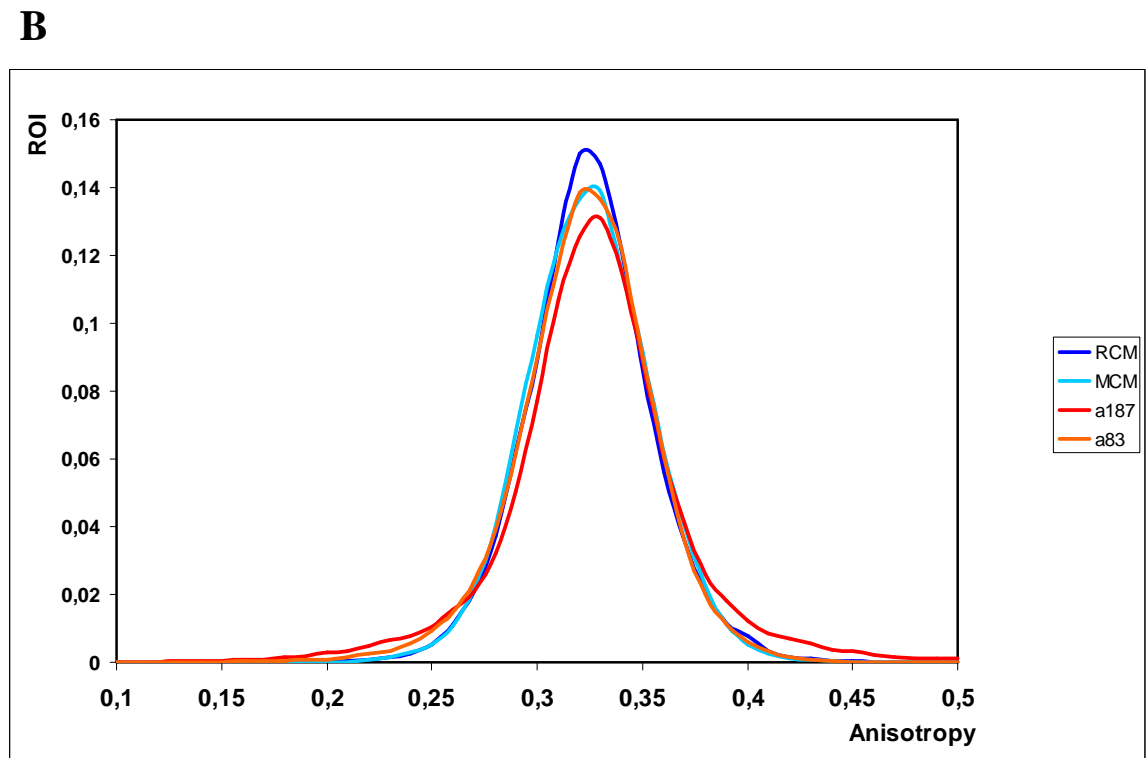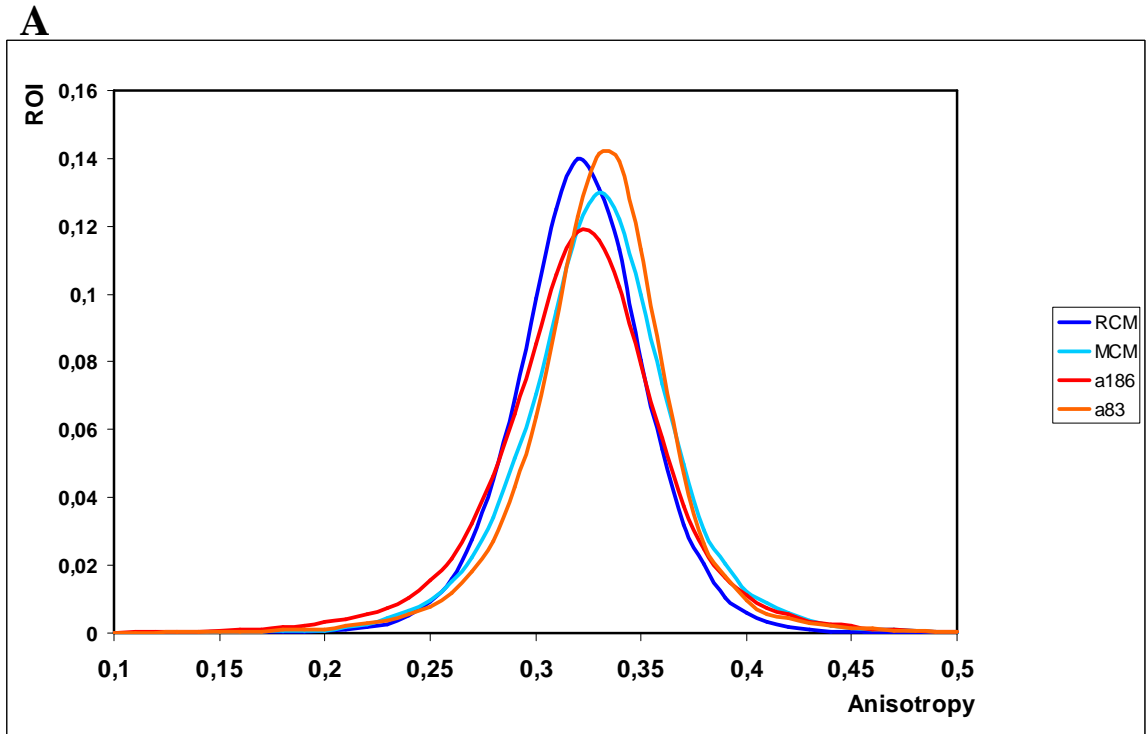
A

B

Figure 20: Anisotropy Distribution in Plasma Membrane. ROIs (cell membrane) were selected from a total of 10 images and total anisotropy measurements plotted with anisotropy over fraction of ROI (1/pixel). Upon stimulation with RCM or a186 GA IV cells show an anisotropy shift towards lower anisotropies when compared to stimulation with control substances MCM and a83 (**A**). No significant change in anisotropy can be observed when GV I cells were stimulated with RCM, a187 or the controls MCM and a83 (**B**).

Discussion

The goal of establishing various tools for the imaging of the Reelin signalling pathway, was a success, in so far as 4 functional, genetically different cell lines containing FP - tagged receptors (CA III, CV VIII, GA IV and GV I) were produced.

Attempts to improve the cell sorting of the receptor - FP fusions to the cytoplasmic membrane using a variety of engineered linkers to separate the receptor from the fluorescence tag did not yield many fruitful results. While intended to localize a greater percentage of the receptors to the membrane, helical linkers in fact led to a higher incidence of aggregation. Furthermore in some cases recognition in western blots was disrupted, potentially indicating wrong protein folding.

Successful simultaneous expression of two differently coloured receptor - fluorescent protein fusion proteins showed the potential to study more than one part of the machinery involved in the Reelin signalling at the same time.

pTagRFP tagged Dab1 associates with Vldlr close to the cytoplasmic membrane directly demonstrating for the first time the interaction of Dab1 with the receptor in unstimulated cells. In cells expressing ApoER2 however, this effect was not seen.

It is possible that the Dab1 association of Vldlr, before binding to Reelin, primes the receptor for signal transduction. Furthermore, it has been shown that membrane localization of Dab1, which is mediated through binding to phosphoinositides (PIs), is a necessary step in the signal transduction[52]. If the Dab1 phosphotyrosine binding (PTB) domain is disrupted, no binding to phosphoinositides occurs, Dab1 no longer associates with the membrane and the signal transduction is actively disrupted.

The concluding hypothesis is that Dab1 binds in ternary complexes with PIs and Vldlr but does not form complexes with ApoER2, prior to stimulation with Reelin. Put together, this indicates that ApoER2 and Vldlr differ in their interaction with Dab 1 in a temporal manner, as Vldlr would be able to transduce the Reelin signal before ApoER2 could.

Experiments using hetero - FRET to observe putative interactions between ApoER2 and Vldlr, through forming of clusters when binding to Reelin, or the binding of Dab1 to ApoER2 \ Vldlr, could be performed using the cell lines expressing FP - tagged variants of ApoER2 \ Vldlr described here.

44

Homo - FRET experiments support that ApoER2 does indeed form dimers or at least closely connected clusters upon the binding of Reelin. However further repetitions are required as the data presented here should be considered little more than a pilot experiment. This could not be shown in the case of the Vldlr, possibly due to it being endocytosed much faster.

In addition homo - FRET experiments in the presence and absence of Dab-1 as a binding partner to the receptor intracellular domain could be attempted. This could potentially give insight into the seemingly dichotomous interactions of Dab1 - phosphorylation and endocytosis of the receptor ligand complex.

Further investigation of the homo - FRET events described here with more sophisticated methods in order to assess cluster size or the percentage of fluorescently tagged receptors would be hard to achieve as the observed effects are very small.

Dimerization of the various components of the Reelin signalling pathway seems to be of vital importance. Not only is oligomerization of either ApoER2, Vldlr or Dab1 in itself capable of stimulating a downstream response[21], but it has recently been shown that Reelin itself needs to form active homo - dimers to function in its signalling role[53].

So similar to the homo - FRET experiments documented in this publication, dimerization of a FP - tagged Dab1 upon stimulation with Reelin in a suitable cell line containing Apoer2 and \ or Vldlr (3T3 A or 3T3 V cells) [49] could be studied as well, as Dab 1 dimerization seems to be sufficient in itself for stimulating downstream targets.[21]

References

1. Nimpf, J. & Schneider, W. J. From cholesterol transport to signal transduction : low density lipoprotein receptor , very low density lipoprotein receptor , and apolipoprotein E receptor-2. *Biochimica et Biophysica Acta* **1529,** 278–298 (2000).

2. Brandes, C. *et al.* Alternative splicing in the ligand binding domain of mouse ApoE receptor-2 produces receptor variants binding reelin but not alpha 2-macroglobulin. *Journal of Biological Chemistry* **276,** 22160–9 (2001).

3. Nimpf, J. & Schneider, W. J. The VLDL receptor: an LDL receptor relative with eight ligand binding repeats, LR8. *Atherosclerosis* **141,** 191–202 (1998).

4. Curran, T. & D'Arcangelo, G. Role of reelin in the control of brain development. *Brain Research Brain Research Reviews* **26,** 285–294 (1998).

5. Rice, D. S. & Curran, T. Role of the Reelin signaling pathway in cetral nervous system development. *Annual Review of Neuroscience* **24,** 1005 – 1039 (2001).

6. D'Arcangelo, G. *et al.* Reelin is a ligand for lipoprotein receptors. *Neuron* **24,** 471–9 (1999).

7. Hiesberger, T. *et al.* Direct binding of Reelin to VLDL receptor and ApoE receptor 2 induces tyrosine phosphorylation of disabled-1 and modulates tau phosphorylation. *Neuron* **24,** 481–9 (1999).

8. Trommsdorff, M. *et al.* Reeler/Disabled-like disruption of neuronal migration in knockout mice lacking the VLDL receptor and ApoE receptor 2. *Cell* **97,** 689–701 (1999).

9. E. Förster, H. H. Bock, J. Herz, X. Chai, M. Frotscher, S. Z. Emerging topics in Reelin function. *European Journal of Neuroscience* **31,** 1511–1518 (2010).

10. Hack, I. *et al.* Divergent roles of ApoER2 and Vldlr in the migration of cortical neurons. *Development* **134,** 3883–91 (2007).

11. Arnaud, L., Ballif, B. a, Förster, E. & Cooper, J. a. Fyn tyrosine kinase is a critical regulator of disabled-1 during brain development. *Current Bology* **13,** 9–17 (2003).

12. Bock, H. H. & Herz, J. Tyrosine kinases in neurons. *Current Biology* **13,** 18–26 (2003).

13. Neural, A. M. *et al.* Scrambler and yotari disrupt the disabled gene and produce a reeler -like phenotype in mice. *Nature* **389,** 1995–1998 (1997).

14. Keshvara, L., Benhayon, D., Magdaleno, S. & Curran, T. Identification of reelin-induced sites of tyrosyl phosphorylation on disabled 1. *Journal of Biological Chemistry* **276,** 16008–14 (2001).

15. Jossin, Y., Ogawa, M., Metin, C., Tissir, F. & Goffinet, A. M. Inhibition of SRC family kinases and non-classical protein kinases C induce a reeler-like malformation of cortical plate development. *Journal of Neuroscience* **23,** 9953–9 (2003).

16. Howell, B. W., Gertler, F. B. & Cooper, J. a. Mouse disabled (mDab1): a Src binding protein implicated in neuronal development. *EMBO Journal* **16,** 121–32 (1997).

17. Beffert, U. *et al.* Functional dissection of Reelin signaling by site-directed disruption of Disabled-1 adaptor binding to Apolipoprotein E Receptor 2: distinct roles in development and synaptic plasticity. *Journal of Neuroscience* **26,** 2041–52 (2006).

18. Howell, B. W., Lanier, L. M., Frank, R., Gertler, F. B. & Cooper, J. a. The disabled 1 phosphotyrosine-binding domain binds to the internalization signals of transmembrane glycoproteins and to phospholipids. *Molecular and Cellular Biology* **19,** 5179–88 (1999).

19. Trommsdorff, M. Interaction of cytosolic adaptor proteins with neuronal Apolipoprotein E Receptors and the amyloid precursor protein. *Journal of Biological Chemistry* **273,** 33556–33560 (1998).

20. Duit, S., Mayer, H., Blake, S. M., Schneider, W. J. & Nimpf, J. Differential functions of ApoER2 and very low density lipoprotein receptor in Reelin signaling depend on differential sorting of the receptors. *Journal of Biological Chemistry* **285,** 4896–908 (2010).

21. Strasser, V. *et al.* Receptor clustering is involved in Reelin signaling. *Molecular and Cellular Biology* **24,** 1378–1386 (2004).

22. Bock, H. H. *et al.* Phosphatidylinositol 3-kinase interacts with the adaptor protein Dab1 in response to Reelin signaling and is required for normal cortical lamination. *Journal of Biological Chemistry* **278,** 38772–9 (2003).

23. Chai, X., Förster, E., Zhao, S., Bock, H. H. & Frotscher, M. Reelin stabilizes the actin cytoskeleton of neuronal processes by inducing n-cofilin phosphorylation at serine3. *Journal of Neuroscience* **29,** 288–99 (2009).

24. Kaminski, C. Quantitative fluorescence microscopy. *Journal of The Royal Society Interface* **6,** S1–S2 (2009).

25. Yan, Y. Analysis of protein interactions using fluorescence technologies. *Current Opinion in Chemical Biology* **7,** 635–640 (2003).

26. Rao, M. & Mayor, S. Use of Forster's resonance energy transfer microscopy to study lipid rafts. *Biochimica et Biophysica Acta* **1746,** 221–33 (2005).

27. Jares-Erijman, E. a & Jovin, T. M. FRET imaging. *Nature Biotechnology* **21,** 1387–95 (2003).

28. Bigelow, C. E., Conover, D. L. & Foster, T. H. Confocal fluorescence spectroscopy and anisotropy imaging system. *Optics Letters* **28,** 695–7 (2003).

29. Marquer, C. *et al.* Influence of MT7 toxin on the oligomerization state of the M1 muscarinic receptor. *Biology of the Cell* **102,** 409–20 (2010).

30. Varma, R. & Mayor, S. GPI-anchored proteins are organized in submicron domains at the cell surface. *Nature* **394,** 798–801 (1998).

31. Sharma, P. *et al.* Nanoscale organization of multiple GPI-anchored proteins in living cell membranes. *Cell* **116,** 577–589 (2004).

32. Tsien, R. Y. The green fluorescent protein. *Annual Review of Biochemistry* **67,** 509–544 (1998).

33. Inouye, S. & Tsuji, F. I. Aequorea green fluorescent protein. Expression of the gene and fluorescence characteristics of the recombinant protein. *FEBS Letters* **341,** 277–280 (1994).

34. Chudakov, D. M., Matz, M. V, Lukyanov, S. & Lukyanov, K. A. Fluorescent proteins and their applications in imaging living cells and tissues. *Physiologicals Reviews* **90,** 1103–1163 (2010).

35. Stephens, D. J. & Allan, V. J. Light microscopy techniques for live cell imaging. *Science* **300,** 82–86 (2003).

36. Patterson, G. H., Knobel, S. M., Sharif, W. D., Kain, S. R. & Piston, D. W. Use of the green fluorescent protein and its mutants in quantitative fluorescence microscopy. *Biophysical Journal* **73,** 2782–2790 (1997).

37. Campbell, R. E. *et al.* A monomeric red fluorescent protein. *Proceedings of the National Academy of Sciences of the United States of America* **99,** 7877–82 (2002).

38. Shu, X., Shaner, N. C., Yarbrough, C. A., Tsien, R. Y. & Remington, S. J. Novel chromophores and buried charges control color in mFruits. *Biochemistry* **45,** (2006).

39. Shaner, N. C., Steinbach, P. a & Tsien, R. Y. A guide to choosing fluorescent proteins. *Nature Methods* **2,** 905–9 (2005).

40. Lippincott-Schwartz, J. & Patterson, G. H. Development and use of fluorescent protein markers in living cells. *Science* **300,** 87–91 (2003).

41. Albertazzi, L., Arosio, D., Marchetti, L., Ricci, F. & Beltram, F. Quantitative FRET analysis with the EGFP-mCherry fluorescent protein pair. *Photochemistry and Photobiology* **85,** 287–97 (2009).

42. Tramier, M., Zahid, M., Mevel, J. & Masse, M. Sensitivity of CFP / YFP and GFP / mCherry pairs to Donor photobleaching on FRET determination by fluorescence

lifetime imaging microscopy in living cells. *Microscopy Research and Technique* **939,** 933–939 (2006).

43. Shcherbo, D. *et al.* Practical and reliable FRET/FLIM pair of fluorescent proteins. *BMC Biotechnology* **9,** 24 (2009).

44. Gautier, I. *et al.* Homo-FRET microscopy in living cells to measure monomer-mimer transition of GFP-tagged proteins. *Biophysical Journal* **80,** 3000–3008 (2001).

45. Bertz, A. *et al.* Mobility of green fluorescent protein in hydrogel-based drug-delivery systems studied by anisotropy and fluorescence recovery after photobleaching. *Macromolecular Bioscience* **13,** 215–26 (2013).

46. Vendruscolo, M., Zurdo, J., MacPhee, C. E. & Dobson, C. M. Protein folding and misfolding: a paradigm of self-assembly and regulation in complex biological systems. *Philosophical transactions. Series A* **361,** 1205–22 (2003).

47. Arai, R., Ueda, H., Kitayama, A., Kamiya, N. & Nagamune, T. Design of the linkers which effectively separate domains of a bifunctional fusion protein. *Protein Engineering* **14,** 529–532 (2001).

48. Evers, T. H., Dongen, E. M. W. M. Van, Faesen, A. C., Meijer, E. W. & Merkx, M. Quantitative Understanding of the Energy Transfer between Fluorescent Proteins Connected via Flexible Peptide Linkers. *Biochemistry* **45,** 13183–13192 (2006).

49. Mayer, H., Duit, S., Hauser, C., Schneider, W. J. & Nimpf, J. Reconstitution of the Reelin signaling pathway in fibroblasts demonstrates that Dab1 phosphorylation is independent of receptor localization in lipid rafts. *Molecular and Cellular Biology* **26,** 19–27 (2006).

50. Stockinger, W. The low density lipoprotein receptor gene family. Differential expression of two alpha 2-macroglobulin receptors in the brain. *Journal of Biological Chemistry* **273,** 32213–32221 (1998).

51. Kuhn, H. & Frank-Kamenetskii, M. D. Template-independent ligation of single-stranded DNA by T4 DNA ligase. *FEBS Journal* **272,** 5991–6000 (2005).

52. Stolt, P. C. *et al.* Phosphoinositide binding by the disabled-1 PTB domain is necessary for membrane localization and Reelin signal transduction. *Journal of Biological Chemistry* **280,** 9671–7 (2005).

53. Cuchillo-ibáñez, I., Balmaceda, V., Botella-lópez, A. & Rabano, A. Beta-amyloid impairs Reelin signaling. *PLOS One* **8,** 1–10 (2013).

Appendix

Zusammenfassung

Der charakteristische *Reeler* Phänotyp and der gut verstandene Reelin Signalweg bilden ein lange etabliertes Modellsystem zur Untersuchung der Entwicklung des Gehirns in Säugetieren.

Apolipoprotein E Rezeptor 2 (ApoER2) und Very Low Density Lipoprotein Receptor (Vldlr) sind wichtige Bestandteile des Reelin Signalweges, da sie mit Reelin interagieren und das Signal weiterleiten. Das Arbeitsmodell für diesen Signalweg ist, dass nach der Bindung an Reelin durch entweder ApoER2 oder Vldlr, letztere ein Dimer bilden, dann Disabled homolog 1 (Dab1) binden, welches selbst dimerisiert und schließlich phosphoryliert wird. Keine dieser Dimerisierungen wurden jemals direkt nachgewiesen.

Im Rahmen dieser Arbeit wurden Zelllinien mit der Expression von Fluoreszenz markierten ApER2 und Vldlr etabliert, um die Mechanismen des Reelin Signalweges auf molekularer Ebene, in lebenden Zellen untersuchen zu können. Insgesamt zehn unterschiedliche Varianten an Fluoreszenzproteinfusionen wurden in Verbindung mit jedem der beiden Rezeptoren entwickelt und produziert. Diese Fusionsproteine wurden in verschiedenen Zelltypen exprimiert und analysiert. Diese Varianten unterscheiden sich durch ihre unterschiedlichen Fluoreszenzproteine (mCherry, EGFP, TagGFP2 oder TagRFP) und durch vier unterschiedliche kleine Linker Sequenzen.

Im speziellen zeigten Hek 293 Zellen mit einer stabilen Expression von TagGFP2 - Fusionsproteinen, wie die Zellinen GA IV (Apoer2) und GV I (Vldlr) die vielversprechendsten Eigenschaften für fluoreszenzmikroskopische Anwendungen.

Mit diesen etablierten Zelllinien konnten spezifesche Interaktionen von fluoreszenzmarkiertem Dab 1 gezeigt werden. Nachdem Dab1 sich mit Vldlr, aber nicht mit ApoER2, in der direkten Umgebung der Zellmembran kolokalisiert.

Des Weiteren wurde die mögliche Dimerisierung oder die Bildung von Clustern der Rezeptoren ApoER2 und Vldlr, während ihrer Interaktion mit Reelin, durch Messung der Anisotropie untersucht. Stimulation mit Reelin verursachte hierbei eine Senkung der Anisotropie in GA IV Zellen, was auf einen möglichen homo - FRET (Förster-Resonanzenergietransfer), aufgrund der Bildung von Clustern von Rezeptoren hinweist. Diese Ergebnisse konnten jedoch nicht unter Verwendung von CV I Zellen nachgewiesen werden. Während noch mehrere Wiederholungen dieser Experimente für definitive

Schlussfolgerungen notwendig sind, können die hier präsentierten Informationen als Indikator dienen, dass Reelin in der Tat das Clustern von ApoER2 verursacht.

Mit den hier vorgestellten molekularen Werkzeugen, können potentiell aufschlussreiche, auf Fluoreszenzmikroskopie basierende Experimente zur Erforschung des Reelin Signalweges durchgeführt werden.

Curriculum vitae

Education and training	
Dates	**September 2006 - 2013**
Principal subjects/occupational skills covered	A441 - Genetics \ Microbiology
Name and type of organization providing education and training	University of Vienna
Level in national or international classification	Aspired Mag. rer. nat in genetics \ microbiology
Dates	**September 2004 – September 2006**
Principal subjects/occupational skills covered	A437 - Biology
Name and type of organization providing education and training	University of Vienna
Level in national or international classification	Primary Diploma Exam (1. Diplomprüfungszeugnis)
Dates	**September 1996 – July 2004**
Principal subjects/occupational skills covered	Secondary School
Name and type of organization providing education and training	BG \ BRG Khevenhüller, Linz
Level in national or international classification	Secondary School Diploma

Acknowledgements